Science of the Total Environment 759 (2021) 143550

Contents lists available at ScienceDirect

Science of the Total Environment

journal homepage: www.elsevier.com/locate/scitotenv

Chromophoric dissolved organic matter in inland waters: Present knowledge and future challenges

Yunlin Zhang [a,b,*], Lei Zhou [a,b], Yongqiang Zhou [a,b], Liuqing Zhang [a], Xiaolong Yao [a,b], Kun Shi [a,b], Erik Jeppesen [c,d,e], Qian Yu [f], Weining Zhu [g]

[a] Taihu Laboratory for Lake Ecosystem Research, State Key Laboratory of Lake Science and Environment, Nanjing Institute of Geography and Limnology, Chinese Academy of Sciences, Nanjing 210008, China
[b] University of Chinese Academy of Sciences, Beijing 100049, China
[c] Department of Bioscience and Arctic Research Centre, Aarhus University, Vejlsøvej 25, DK-8600 Silkeborg, Denmark
[d] Sino—Danish Centre for Education and Research, Beijing 100190, China
[e] Limnology Laboratory, Department of Biological Sciences and Centre for Ecosystem Research and Implementation, Middle East Technical University, Ankara, Turkey
[f] Department of Geoscience, University of Massachusetts, Amherst, MA, USA
[g] Ocean College, Zhejiang University, Zhoushan, Zhejiang, China

HIGHLIGHTS

- FT-ICR-MS can provides more composition information than optical and isotope techniques.
- The photochemical degradation and microbial decomposition are the underlying mechanisms of CDOM cycle.
- CDOM dynamics is challenging due to the high complexity, heterogeneity, and rapid turnover.
- CDOM numerical models is required to understand CDOM dynamics and climate feedbacks.

GRAPHICAL ABSTRACT

Environment roles of CDOM in inland waters

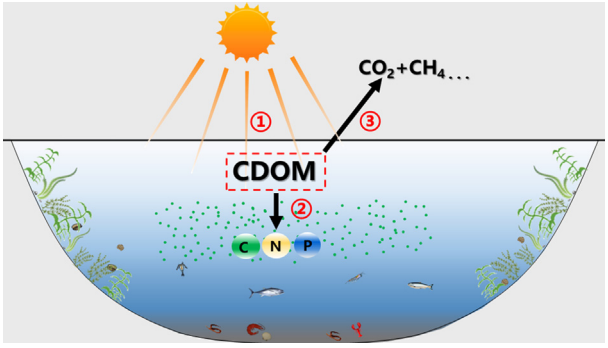

ARTICLE INFO

Article history:
Received 5 August 2020
Received in revised form 1 November 2020
Accepted 2 November 2020
Available online 17 November 2020

Editor: Prof. Ashantha Goonetilleke

Keywords:
Absorption coefficient
Chromophoric dissolved organic matter
Inland waters
Microbial decomposition
Remote sensing

ABSTRACT

Chromophoric dissolved organic matter (CDOM) plays an important role in the biogeochemical cycle and energy flow of aquatic ecosystems. Thus, systematic and comprehensive understanding of CDOM dynamics is critically important for aquatic ecosystem management. CDOM spans multiple study fields, including analytical chemistry, biogeochemistry, water color remote sensing, and global environmental change. Here, we thoroughly summarize the progresses of recent studies focusing on the characterization, distribution, sources, composition, and fate of CDOM in inland waters. Characterization methods, remote sensing estimation, and biogeochemistry cycle processes were the hotspots of CDOM studies. Specifically, optical, isotope, and mass spectrometric techniques have been widely used to characterize CDOM abundance, composition, and sources. Remote sensing is an effective tool to map CDOM distribution with high temporal and spatial resolutions. CDOM dynamics are mainly determined by watershed-related processes, including rainfall discharge, groundwater, wastewater discharges/effluents, and biogeochemical cycling occurring in soil and water bodies. We highlight the underlying mechanisms of the photochemical degradation and microbial decomposition of CDOM, and emphasize that photochemical and microbial processes of CDOM in inland waters accelerate nutrient cycling and regeneration in the water

* Corresponding author at: Nanjing Institute of Geography and Limnology, Chinese Academy of Sciences, 73 East Beijing Road, Nanjing 210008, China.
E-mail addresses: ylzhang@niglas.ac.cn (Y. Zhang), yqzhou@niglas.ac.cn (Y. Zhou), xlyao@niglas.ac.cn (X. Yao), kshi@niglas.ac.cn (K. Shi), ej@bios.au.dk (E. Jeppesen), qyu@geo.umass.edu (Q. Yu), zhuwn@geo.umass.edu (W. Zhu).

https://doi.org/10.1016/j.scitotenv.2020.143550

column and also exacerbate global warming by releasing greenhouse gases. Future study directions to improve the understanding of CDOM dynamics in inland waters are proposed. This review provides an interdisciplinary view and new insights on CDOM dynamics in inland waters.

Contents

1. Introduction

Dissolved organic matter (DOM) in aquatic environments is a complex mixture of carbon, nitrogen, phosphorus, and sulfur-containing molecular fragments with molecular weights ranging from a few hundred to 100,000 Da (Da). Chromophoric DOM (CDOM), also known as gelbstoff, gilvin, yellow substance, or colored dissolved organic matter, is mainly composed of aromatic amino acids, lignin phenols, and undefined humic substances and shows distinct bioavailability differences due to its complex sources, compositions and molecular structures (Hansell and Carlson, 2015; Nebbioso and Piccolo, 2013; Nelson and Siegel, 2013; Zark and Dittmar, 2018).

CDOM is closely related to the biogeochemical cycle and energy flow of ecosystems, and its changes are of vital importance by promoting transformation and evolution of aquatic ecosystems (Lapierre et al., 2013; Williams et al., 2016; Wilson and Xenopoulos, 2009). Studies associated with the characterization, source, composition, temporal and spatial patterns, degradation, transformation, and environmental effects of CDOM are inherently complex and interdisciplinary. The major environmental roles of CDOM can be categorized into three items (Fig. 1): 1) Light-absorbing CDOM largely determines the optical properties of water bodies and underwater ultraviolet and blue light attenuation, being of particular importance in alpine and (Ant)Arctic oligotrophic waters or humic-rich lakes (Huovinen et al., 2003; Laurion et al., 2000; Zhang et al., 2011c). CDOM may also protect aquatic organisms by reducing both the amount and the penetration depth of harmful UV-B (280–320 nm) radiation (Laurion et al., 2000; Williamson et al., 2014). In addition, CDOM absorption in the blue light region overlaps with that of phytoplankton chlorophyll-*a* and non-phytoplankton suspended particles, affecting the quantitative remote sensing retrieval of the concentrations of optically active substances in water bodies (Dierssen, 2010; Gitelson et al., 2007; Odermatt et al., 2012). 2) The transformation of CDOM is accompanied by biogeochemical cycles of several biogenic elements such as carbon, nitrogen, and phosphorus (Wear et al., 2015; Zhang et al., 2011a). Therefore, CDOM is an important link in the nutrient availability and regeneration processes supporting bacterial and phytoplankton growth in aquatic ecosystems (Mladenov et al., 2011; Zhang et al., 2009b); 3) CDOM represents a key component of the global carbon pool. The source, composition, degradation, and mineralization of CDOM are involved in the global carbon cycle and carbon budget (Battin et al., 2009; Zhou et al., 2018b), potentially leading to greenhouse gas emissions and affecting global climate change (Emilson et al., 2018; Lapierre et al., 2013).

Under the influence of global climate change, eutrophication and intensified disturbances from human activities over the past four decades have resulted in increased export of terrestrial and anthropogenic CDOM to downstream receiving aquatic ecosystems (Drake et al., 2018; Kothawala et al., 2014; Massicotte et al., 2017). The degradation and mineralization of CDOM have, in turn, directly or indirectly affect the structure and function of the aquatic ecosystems downstream. Studies of CDOM-related issues have quickly increased over the past 20 years, now being a hotspot in the fields of remote sensing, aquatic ecology, and the global carbon cycle. CDOM is involved in multiple

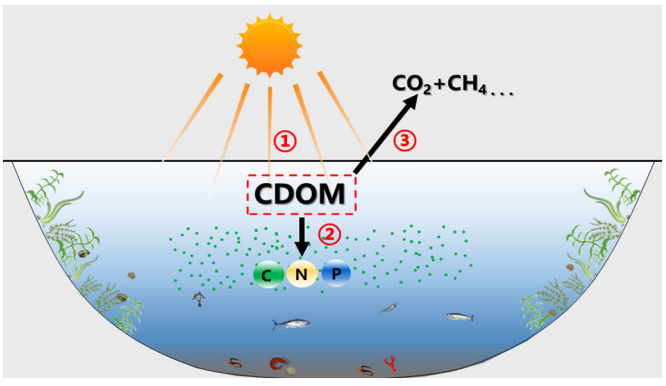

Fig. 1. Environment roles of CDOM in inland waters ①: Light attenuation effects; ②: biogeochemical cycles effects; ③: greenhouse gas emissions effects.

study fields, including analytical chemistry, water optics and water color remote sensing, biogeochemical cycles in natural ecosystems, coagulation efficiency, disinfection byproduct formation, membrane fouling, and oxidant demand in engineered systems (Ike et al., 2019; Kutser et al., 2005; Laurion et al., 2000; Lavonen et al., 2015; Murphy et al., 2013; Nebbioso and Piccolo, 2013).

Many reviews focus on DOM/CDOM characterization techniques, key processes, and marine environments (Chen et al., 2019a; Dittmar and Stubbins, 2014; Ike et al., 2019; Ishii and Boyer, 2012; Li and Hur, 2017; Mopper et al., 2007; Nelson and Siegel, 2013; Perdue and Ritchie, 2003). Comparatively, little systematic effort has been made to summarize the sources, composition, fate, and environmental effects of CDOM in inland waters, which may reflect that it is a complex issue that have to deal with high temporal and spatial heterogeneities, multi-disciplinarity and so far insufficient attention to the importance of CDOM. This is unfortunate as the global annual emissions of carbon dioxide from inland waters to the atmosphere are similar in magnitude to the carbon dioxide uptake by the oceans, and the global burial of organic carbon in inland waters sediments exceeds organic carbon sequestration on the ocean floor (Tranvik et al., 2009), even though inland waters cover on average only 3% of the global continental area (Downing et al., 2006). Because of the predominant role of CDOM in dissolved organic carbon (DOC) and the vital binding roles of CDOM with nutrients (de Matos Valerio et al., 2018; Griffin et al., 2018; Mesfioui et al., 2015; Zhang et al., 2011a; Zhang et al., 2018), it is urgent to better understand CDOM dynamics in inland waters. Therefore, a comprehensive and multi-disciplinary review of CDOM studies could advance our understanding of CDOM dynamics.

In this review, we thoroughly summarize CDOM characterization methods, remote sensing estimations, temporal-spatial distribution, sources, and composition dynamics from four aspects: 1) CDOM characterization techniques and methods; 2) CDOM remote sensing estimation model and application; 3) CDOM patterns, sources, and driving factors; and 4) CDOM transformation mechanisms and environmental effects. We aim to provide a guideline for CDOM researchers from a comprehensive and interdisciplinary perspective to promote a better understanding of the importance and implications of CDOM cycling in inland waters.

2. Overview of CDOM and DOM from the bibliometric perspective

To elucidate the study interest differences in the CDOM and DOM field and popular topics of CDOM, author keywords from the bibliometric perspective were analyzed. The online version of the Science Citation Index (SCI) Expanded was searched using the keywords (TS = CDOM, TS = DOM) as the topic to compile a bibliography of all papers related to the study of CDOM and DOM. The keywords with the same meanings were unified into one word, and publications that lacked author keywords were not included in this analysis. In addition, we excluded CDOM and DOM in the keyword analysis because CDOM and DOM was used as our search term.

The 50 most frequently used keywords showed that the CDOM study covered three main directions (Fig. S1): 1) characterization methods including absorption, fluorescence, the excitation-emission matrix (EEM), and parallel factor analysis (PARAFAC); 2) water color remote sensing including remote sensing, ocean color, optical properties, and MODIS; and 3) biogeochemistry cycle processes including DOM, DOC, chlorophyll, and photochemistry. Obviously, many keywords related to water color and remote sensing are recorded, which is specific to CDOM. Therefore, CDOM remote sensing is extensively reviewed in our study. The bibliometric analysis showed that CDOM study covered the multidisciplinary fields needing multiscale interdisciplinary processes, mechanisms, and models understanding. In contrast, other high-frequency keywords including humic substances, adsorption, humic acid, mercury, copper were recorded for DOM study indicating different study topics (Fig. S2). Especially, the high-frequency keywords of mercury, copper, and heavy metals show the environmental role of DOM metal contaminants, which is seldom reported for CDOM.

3. CDOM characterization techniques and methods

3.1. UV–vis spectroscopy

In practice, filtrate passing through a submicron filter (usually 0.22 μm) is normally used for CDOM characterization to eliminate the scattering effect of the small particles <0.45 μm but larger than 0.22 μm compared to DOM. Because CDOM consists of a mixture of substances with different sources and complex chemical compositions, it is difficult to quantify CDOM in terms of mass or concentration. We further operationally define the quantity of CDOM by its Napierian absorption coefficient at a reference wavelength. Absorption coefficients at characteristic wavelengths (254, 280, 350, 375, or 440 nm) measured by absorption spectroscopy and DOC concentration were used as proxies for the concentration or abundance of CDOM in many studies (Table S1) (Griffin et al., 2018; Massicotte et al., 2017; Spencer et al., 2012; Stedmon et al., 2000; Zhang et al., 2011a; Zhang et al., 2018). The absorption coefficient of CDOM has high spatial variation as evidenced by $a(254)$ ranging from 0.011 m^{-1} to 695 m^{-1} (Zhang et al., 2018), while $a(350)$ ranged from 0.01 m^{-1} to 1839 m^{-1} (Massicotte et al., 2017). In drinking water and wastewater treatment studies, $a(254)$ and associated specific ultraviolet absorbance were widely used to characterize CDOM abundance and aromatic compounds (Lavonen et al., 2015; McKnight et al., 2001). $a(320)$ was used to correlate the diffuse attenuation coefficient for UV-B radiation (280–320 nm) to elucidate the effects of CDOM on ultraviolet radiation (UVR) attenuation (Laurion et al., 2000; Morris et al., 1995). $a(350)$ was often used to characterize CDOM concentration and biogeochemical cycles in lakes and rivers (Lambert et al., 2016; Osburn et al., 2011). In contrast, $a(440)$ was used to estimate the CDOM concentration in water color remote sensing studies because satellite ocean color sensors have a spectral channel near 440 nm (Olmanson et al., 2016; Zhu et al., 2011). Therefore, the absorption coefficient at different wavelengths used in different studies created difficulty and uncertainty in the accuracy of the global comparison of CDOM in inland waters. Considering that $a(254)$ mainly reflects aromatic compounds and $a(440)$ is often near 0 or negative for clear water due to low instrument detection limits, we suggest that in future studies more researchers should use $a(350)$ to characterize CDOM concentration to facilitate further comparison. In addition, there were significant positive correlations between the DOC concentration and CDOM absorption in inland waters (Brezonik et al., 2015; Griffin et al., 2018; Massicotte et al., 2017; Song et al., 2017), which indicated that DOC was a reliable and regional proxy for CDOM characterization. However, highly variable linear regression slopes have been found between DOC concentrations and CDOM absorptions in inland waters with different water color characteristics, which highlights that a classification of water color is required before estimating CDOM using DOC concentration in optically complex inland waters.

Additionally, the specific ultraviolet absorbance $SUVA_{254}$ (ratio of the UV absorption coefficient at 254 nm to the DOC concentration) (Griffin et al., 2018; Spencer et al., 2012; Weishaar et al., 2003), spectral slope S (Stedmon et al., 2000; Zhang et al., 2011b), spectral slope ratio S_R (Helms et al., 2008), and the relative molecular weight parameter M (De Haan and De Boer, 1987) are also widely used for semi-quantitative characterization of CDOM sources and composition (Table S1). $SUVA_{254}$ is positively proportional to the degree of aromaticity of CDOM, further indicating an increasing input from terrestrial sources with high SUVA values (Weishaar et al., 2003; Zhou et al., 2016). In contrast, the values of S, S_R, and M increase with decreasing molecular size and humification of CDOM (Helms et al., 2008). Overall, DOC concentrations and CDOM absorption coefficients are positively correlated with $SUVA_{254}$ and negatively correlated with S, S_R, and M values (Helms et al., 2008; Zhang et al., 2011b). These results indicate that enhanced

input of terrestrial humic-rich CDOM can result in increasing $SUVA_{254}$ and decreasing S, S_R, and M values.

3.2. Fluorescence spectroscopy

Fluorescence DOM (FDOM) is a fraction of CDOM that can emit fluorescence when excited at short wavelengths. Fluorescence spectroscopy, especially the EEM technique, is widely utilized to characterize the sources and composition of CDOM due to its high sensitivity, high information content, low cost, and absence of influence on the sample (Chen et al., 2003; Coble, 1996; Li and Hur, 2017; Stedmon and Markager, 2005). Regions of three-dimensional EEM can be assigned to different classes of fluorescence compounds. Early on, the position, height, and fluorescence ratio of EEM spectra peaks were mainly determined by the "peak picking" technique (Coble, 1996; Stedmon et al., 2003), which can be misleading due to spectral overlap, interactive interference, and subjective factors. Parallel Factor Analysis (PARAFAC) is now commonly utilized to analyze EEM data. PARAFAC is an alternating least-squares algorithm that splits each EEM into a series of tri-linear components and a residual array (Murphy et al., 2013; Stedmon and Bro, 2008; Stedmon et al., 2003), and it can objectively and accurately decompose complex EEMs into independent fluorescent components that represent groups of similar fluorophores, including humic-like, fulvic-like, tyrosine-like, and tryptophan-like components (Ishii and Boyer, 2012; Zhang et al., 2009b). However, one of the most critical issues for PARAFAC model results and explanation is the lack of required rigorous dataset. The recommended minimum sample number for EEM-PARAFAC analysis in several PARAFAC method studies is approximately or >60 (Murphy et al., 2013; Murphy et al., 2018; Stedmon and Bro, 2008), but it turned out that many reported PARAFAC-derived fluorescent components in the literature are based on a small dataset, sometimes including <10 samples. In addition, the controversial number of fluorescence components and fluorescence spectra derived from PARAFAC obscure the correlations between the fluorescence components and physicochemical properties, an issue requiring further investigation and mechanism analysis. In addition, there is a tendency to over-interpret fluorescence information fitted from mathematical models without solid physical and chemical mechanisms. A recent meta-analysis of 90 peer-reviewed PARAFAC models revealed no clear connection between fluorescence spectral composition and DOM/CDOM biogeochemistry, indicating certain fluorescence components reoccur regardless of sample source (Wünsch et al., 2019). This result may be attributed that physicochemical reactions act upon DOM to produce a set of highly conserved fluorescence spectra (Wünsch et al., 2019). Therefore, multidetector analysis to the interpretation of fluorescence and linking fluorescence components with complementary physical and chemical information are recommended to the interpretation of PARAFAC results and better understanding the biogeochemistry of CDOM fractions (Cuss and Gueguen, 2015; Romera-Castillo et al., 2014).

In addition to EEM coupling with PARAFAC, the fluorescence index (FI) (McKnight et al., 2001), humification index (HIX) (Zsolnay et al., 1999), biological index (BIX) (Huguet et al., 2009), and fluorescence peak ratio index (FPRI) (Zhou et al., 2017) have also been proposed to semi-quantitatively distinguish the sources and composition of CDOM (Table S1). FI with a value of ~1.9 indicates microbially derived sources and a value of ~1.4 indicates terrestrially derived materials (McKnight et al., 2001). Actually, an increasing number of studies have shown that FI defined as a mixed value did not add extra information to identify the composition of CDOM sources. While the humification degree of CDOM increases, the ratio of hydrogen to carbon will decrease, and the emission spectrum of fluorescent molecules will experience a red-shift, resulting in a higher value of HIX (Zsolnay et al., 1999). BIX reflects the proportion of newly generated CDOM in the overall CDOM pool, and a value of 1 or higher indicates strong biological activity or predominant autochthonous CDOM (Huguet et al., 2009). FPRI, which is defined as the integral ratio of the fluorescence peak C (E_x: 320–360 nm, E_m: 420–480 nm) to the peak T (E_x: 225–230 nm and 275 nm, E_m: 345–350 nm), can track the composition dynamics and the relative contributions of autochthonous and allochthonous sources of CDOM (Zhou et al., 2017). Similar to PARAFAC fluorescence components, some inconsistent results from different fluorescence indices were often observed. In addition, it is difficult to accurately identify the changes in CDOM sources and composition based on these several fluorescence indices because they cover a small variability.

3.3. Stable isotope

Stable isotopic composition of DOM, including δ^{13}C-DOC and δ^{15}N-total dissolved nitrogen used for bulk DOM (Table S1), has been used to trace the sources and transformation processes of CDOM in various aquatic ecosystems (Goldberg et al., 2015; Osburn et al., 2011; Stedmon et al., 2015; Zhou et al., 2018a). For instance, allochthonous CDOM with diluted δ^{13}C has a value ranging from −29‰ to −26‰, while autochthonous CDOM with rich δ^{13}C-DOC has a value ranging from −24‰ to −20‰ (Hood et al., 2009; Spencer et al., 2014). Isotopic analyses of DOC showed that the younger portion (^{14}C-enriched) of terrestrial organic matter is selectively degraded compared with the older DOM (^{14}C-depleted) (Raymond and Bauer, 2001). Stable isotopic δ^2H and δ^{18}O in inland waters can provide information about hydrological processes, including flow, evaporation, water supply, and hydrological connectivity, and thereby characterize the transformation of DOM. For example, evaporation fuels the accumulation of heavier isotopic water molecules (H^2HO and $H_2^{18}O$) in surface water, and δ^2H and δ^{18}O can therefore be used to trace the sources of riverine- or groundwater-derived CDOM in lake ecosystems (Zhou et al., 2018b). Over recent decades, compound-specific isotope analysis (CSIA), especially through measuring δ^{13}C, δ^{15}N, and ^{14}C in specific organic compounds, has further advanced our understanding of DOM/CDOM sources (Glibert et al., 2019; Osburn et al., 2011). In addition, biomarkers (*e.g.*, lipid and lignin) in combination with absorption and fluorescence spectroscopy as well as stable isotopes provide a more comprehensive picture of CDOM composition and sources (Osburn et al., 2011).

3.4. Fourier transform ion cyclotron resonance mass spectrometry

Recent advances, especially the development of ultrahigh resolution mass spectrometry, have improved our understanding of the molecular characterization of CDOM. A growing number of studies have been carried out using Fourier transform ion cyclotron resonance mass spectrometry (FT ICR-MS) coupled with electrospray ionization to identify CDOM composition at a molecular level. Kendrick and van Krevelen plots can be firstly used to classify the assigned molecular formulas into different categories, including lipids, proteins and amino sugars, carbohydrates, unsaturated hydrocarbons, lignins, tannins, and condensed aromatics (Dittmar et al., 2012; Kellerman et al., 2014; Ohno et al., 2014; Riedel and Dittmar, 2014; Singer et al., 2012; Sleighter and Hatcher, 2007; Ward et al., 2017) (Fig. 2). Recently, a widely used method of solid-phase are recommended to be classified according to the O/C and H/C ratios and a modified quantitative aromaticity index (AImod) into polycyclic condensed aromatics (AImod >0.66), polyphenolic (0.66 ≥ AImod >0.5), highly unsaturated and phenolic (AImod ≤0.50 and H/C < 1.5), aliphatic (2.0 > H/C ≥ 1.5 and $N = 0$), peptide-like (2.0 > H/C ≥ 1.5 and $N > 0$), and sugar-like compounds (H/C ≥ 1.5 or O/C > 0.9) (Coward et al., 2019; Kellerman et al., 2020; Spencer et al., 2014). In addition, FT ICR-MS tracing molecular composition changes can be widely used to elucidate the sources and cycle processes of DOM/CDOM (Kellerman et al., 2015; Lee et al., 2019; Stubbins et al., 2010). For example, FT ICR-MS revealed that photobleaching of CDOM resulted in the loss of aromatics and a reduction of molecular diversity. In detail, black carbon and carboxylic-rich alicyclic molecules were photo-resistant, aromatic compounds including the lignin, tannin, and

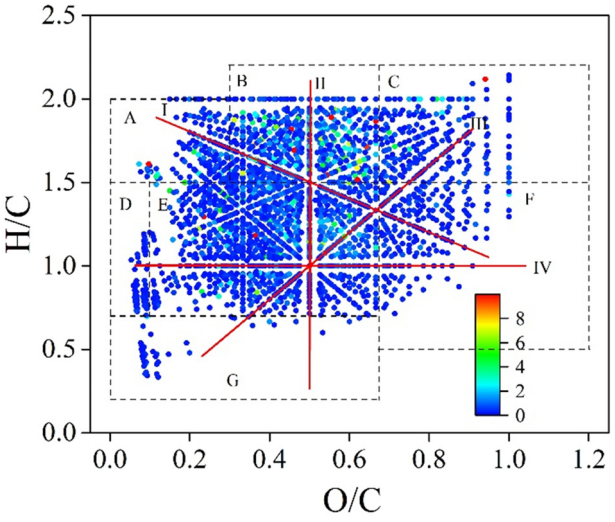

Fig. 2. van Krevelen diagram for Lake Taihu CDOM sample from the molecular level measured using a 15 T FT-ICR mass spectrometer (solariXTM system, Bruker Daltonics, Billerica, MA). A: lipids, B: proteins, C: carbohydrates; D: unsaturated hydrocarbons, E: lignins, F: tannins, G: condensed aromatics. The distinctive lines denote the following chemical reactions: (I) methylation/demethylation or alkyl chain elongation; (II) hydrogenation/dehydrogenation; (III) hydration/condensation; and (IV) oxidation/reduction.

aromatic being the most photoreactive, and the photo-produced pool was dominated by aliphatic compounds (Stubbins et al., 2010). Kellerman et al. (2015) concluded that intrinsic molecular properties were an important control of overall organic matter reactivity by combining ultrahigh-resolution mass spectrometry and optical spectroscopy to investigate the persistence of DOM in lakes related to its molecular characteristics (Kellerman et al., 2015).

More importantly, FT-ICR-MS can accurately differentiate small differences in the molecular masses of CDOM components due to ultrahigh mass resolution and a mass accuracy below 1 ppm. When slight CDOM and DOC variabilities cannot be detected with the commonly used composition parameters S, S_R, and SUVA, FT-ICR-MS can clearly observe these slight changes. However, with only empirical formulae, although systematized in Kendrick and van Krevelen plots, information about the chemical structure of CDOM compositions remains rather poor. Therefore, the content and structures of polycyclic condensed aromatics, polyphenolic, highly unsaturated and phenolic, aliphatic, peptide-like, and sugar-like compounds must be better characterized to enable understanding of the genesis, structure, and chemical reactivity of DOM. Unfortunately, though, the limited availability of FT-ICR-MS and high price of CDOM molecular characterization block most researchers. In addition, the pre-processing of raw mass spectra obtained from FT-ICR-MS, including inner-calibration and molecular formulae assignments, needs sophisticated analytical chemistry and data analysis to accurately extract CDOM molecular information. Therefore, strategies for low-cost FT-ICR-MS measurements and reliable data processing are among the greatest challenges for future studies. Moreover, a widely used method of solid-phase extraction with modified styrene divinyl benzene polymer type sorbents (PPL, ENV) extracts >60% of coastal and > 40% of deep-sea DOC (Dittmar et al., 2008). Improving the extraction efficiency before FT-ICR-MS detection, in order to avoid information loss, is also a great challenge that needs to be considered and studied further in the future.

3.5. Other methods

Nuclear magnetic resonance (NMR) (Miller et al., 2009; Nebbioso and Piccolo, 2013; Zark and Dittmar, 2018), two dimensional correlation spectroscopy (2DCOS) (Chen et al., 2019a), and high-performance size exclusion chromatography (HPSEC) (Wu et al., 2003; Wünsch et al., 2018) are also used to characterize the source, composition, and molecular weight of CDOM, factors that require more focus in future studies. Recently, *in situ* CDOM fluorescence sensors, such as the Cyclops 7 (Turner Designs, USA), the ECO FL CDOM fluorometer (Wetlabs, USA), the MicroFlu-CDOM fluorometer (Trios GmbH, Germany), the UV fluorometer (SeaPoint), and the EXO2 FDOM sensor (YSI, USA), have been widely used to monitor the high frequency variation and understand the short term rapid biogeochemistry processes of CDOM (Mihalevich et al., 2017; Ruhala and Zarnetske, 2016; Wymore et al., 2018).

3.6. Combination of more advanced analytical methods and techniques

The use of state-of-the-art techniques, including FT-ICR-MS and NMR, has ensured great breakthroughs in our understanding of the sources and composition of CDOM at molecular level. However, most techniques still only offer semi-quantitative information. By combining CDOM characterization techniques, including traditional ultraviolet-visible absorption spectroscopy, EEMs, 2DCOS, stable isotopes, and newly developed FT-ICR-MS and NMR, more accurate information on the abundance, chemical structure, composition, and sources of CDOM could be acquired, and the underlying driving mechanisms of CDOM dynamics might be elucidated more clearly. It is vitally important to develop some standard procedures for distinguishing CDOM sources, structures, and compositions based on absorption spectroscopy, EEMs, stable isotopes, and FT-ICR-MS and NMR experimental data.

4. Remote sensing retrieval of CDOM

Elucidating the distribution and dynamics of CDOM is crucial for monitoring, assessing, and managing inland waters (Keith et al., 2002; Kutser et al., 2005; Massicotte et al., 2017; Siegel et al., 2002; Zhang et al., 2018). In addition to the *in situ* sampling and measurement of CDOM, remote sensing is considered an important supplement or substitute to obtain an overview of the temporal-spatial patterns of CDOM due to its unparalleled advantages of collecting measurements from historical and large-scale perspectives (Joshi et al., 2017; Matthews, 2011; Swan et al., 2013; Wen et al., 2019). Remote sensing of surface water color depends on the use of spectral channels that provide radiometric information at a few selected wavelengths about the light backscattered from the upper layer of the water, which is known as remote sensing reflectance (Maritorena et al., 2002; Wen et al., 2019). Compared with other optically active substances, such as total suspended matter and chlorophyll-*a*, it is more difficult to obtain an accurate estimation of CDOM from satellite data due to its low optical signals and absorption spectral shapes that are similar to those of non-phytoplankton particulate matter.

Much effort has been directed at developing a series of empirical, semi-empirical, and semi-analytical algorithms to estimate CDOM and improve the estimation accuracy for inland waters (Fig. 3). First, several empirical relationships have been established between the CDOM absorption coefficient and remote sensing reflectance. Recently, also machine learning methods such as regularized linear regression (RLR), random forest regression (RFR), kernel ridge regression (KRR), Gaussian process regression (GPR), artificial neural networks (ANN), and support vector machines (SVM) have been used to estimate CDOM absorption without considering the differences in water optical properties (Ruescas et al., 2018; Zhao et al., 2018). Second, several semi-empirical algorithms considering band ratios have been proposed as predictive models for estimating CDOM from spectral data in different waters around the world (Zhu et al., 2011). Third, the semi-analytical QAA-CDOM algorithm, an improved and optimized version of a quasi-analytical algorithm (QAA), has been applied to estimate CDOM absorption in different riverine, lake, estuarine, and coastal waters (Li et al.,

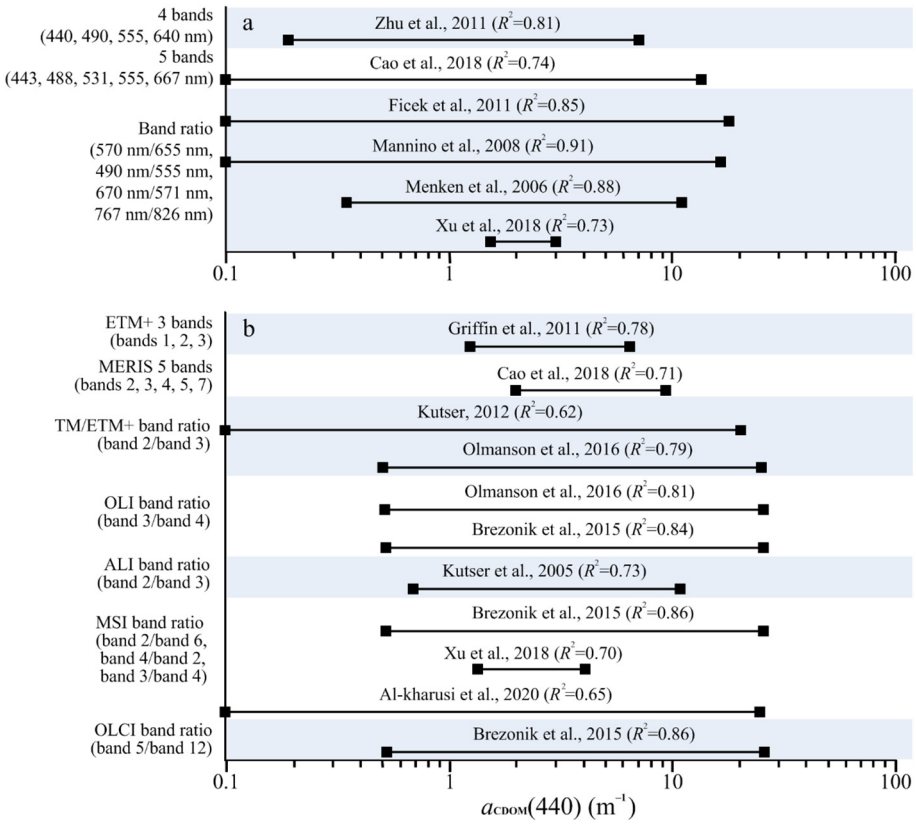

Fig. 3. Overview of retrieval models of $\alpha(440)$ from a) field spectral reflectance measurements using the 4 band combination and b) satellite imagery using the ETM+ 3 band, the TM/ETM + band ratio, the OLI band ratio, the ALI band ratio, the MSI band ratio, and the OLCI band ratio (Al-Kharusi et al., 2020; Brezonik et al., 2015; Cao et al., 2018; Ficek et al., 2011; Griffin et al., 2011; Kutser, 2012; Kutser et al., 2005; Mannino et al., 2008; Menken et al., 2006; Olmanson et al., 2016; Xu et al., 2018; Zhu et al., 2011).

2018). In addition, another semi-analytical algorithm, shallow water bio-optical properties (SBOP), has been developed and successfully used to estimate spatial and temporal patterns of CDOM absorption for both optically shallow and deep waters by eliminating bottom effects (Li et al., 2017; Li et al., 2018). These semi-analytical algorithms made a significant improvement to avoid location dependency by resolving CDOM optical properties based on bio-optical radiative transfer models. Based on the above-mentioned CDOM estimation algorithms, many different satellite imageries such as Landsat, Sentinel-2, MERIS, and Hyperion have been widely used over the past decade to remotely map CDOM in a number of optically complex inland waters (Li et al., 2018). Overall, the band ratio is the most common algorithm, and the Landsat series satellite is the most useful remote sensing data covering $a(440)$ values from <0.1 to >20 m^{-1} (Fig. 3). Meanwhile, several CDOM composition parameters, water quality and water environment indicators related to CDOM have been estimated using remote sensing methods based on different satellite data (Cao and Miller, 2015; Cao et al., 2018; Chen et al., 2019b; de Matos Valerio et al., 2018; Miao et al., 2019).

Most algorithms of CDOM remote sensing estimation are empirical or semi-empirical (Fig. 3) (Cao et al., 2018; Kutser et al., 2005; Olmanson et al., 2016), which inhibits their application to other complex optical properties of inland waters without synchronous CDOM measurements. More importantly, the current many satellite instruments have no special spectral channels for CDOM remote sensing (Brezonik et al., 2015). In addition, the use of satellite images for mapping long-term CDOM dynamics with both high spatial (≤ 10 m) and temporal (≤ 1 day) resolutions in inland waters is problematic (Al-Kharusi et al., 2020; Olmanson et al., 2016; Xu et al., 2018). Therefore, the new generation of satellite ocean color sensors should be specifically designed to characterize CDOM and its spectral dependence in inland waters. CDOM information from remote sensing with sufficient precision and temporal and spatial resolutions allows us to elucidate highly dynamic physical and biological processes and quantify the CDOM biogeochemical cycle in inland waters.

CDOM dynamics in inland waters are linked to complicated factors, including solar radiation, topography, hydrology, and ambient ecological environments (Aulló-Maestro et al., 2017; Evans et al., 2017; Haaland et al., 2010; Helms et al., 2008; Zhou et al., 2016). Thus, in-depth understanding relies on analyses of long-term observations and data covering large spatial and temporal scales. A complementary approach to expand the spatial and temporal scales of CDOM studies is the use of *in situ* bio-optical sensors and remote sensing monitoring. More attention and effort must be paid to satellite observations at different temporal and spatial resolutions that can provide a synoptic view of the CDOM dynamics from a historical viewpoint over a large spatial scale. Therefore, the new generation of satellite ocean color sensors should be designed to characterize CDOM and its spectral dependence in inland waters to facilitate global comparisons. Moreover, CDOM fluorescence bio-optical sensors can be used for *in situ* monitoring of CDOM dynamics at high temporal resolution (minutes) to obtain a better understanding of short-term driving processes (Mihalevich et al., 2017; Ruhala and Zarnetske, 2016; Wymore et al., 2018). Meanwhile, more *in situ* CDOM observation data acquired by these sensors will further improve the precision of CDOM remote sensing algorithms. Combining the high frequency *in situ* CDOM observation and large spatial scale CDOM remote sensing estimation will deep our understanding of CDOM source, key driving processes, and environmental effects (Juhls et al., 2019).

Remote sensing estimation of CDOM is still challenging for inland waters because the absorption spectra of CDOM in the blue region are overlapping with the high absorption of suspended particles (Xu et al.,

2018). CDOM estimation algorithms developed for specific study sites based on a small dataset covering a limited CDOM range might not be directly applicable to other inland waters, as it may result in low precision and high uncertainty. In addition, inorganic components such as iron can easily influence water color in inland waters (Xiao et al., 2015), which may result in the misleading of CDOM estimation. Therefore, more studies are needed in order to develop more robust models to improve CDOM estimation precision to increase our understanding of CDOM dynamics.

5. CDOM patterns, sources and driving factors

A recent study showed that the CDOM distribution displays high spatial heterogeneity with $a(440)$ of CDOM, ranging up to ~40 m^{-1} or more in inland waters (Brezonik et al., 2015). To compare and present the global distribution of CDOM absorption coefficients in inland waters, we collected the available CDOM absorption coefficient in inland waters from the literature (Table S2). Unfortunately, CDOM absorption coefficients at different wavelengths were used due to the individual aim of the different studies, typically including 254, 280, 320, 350, and 440 nm *etc.* To facilitate comparison, we therefore had to develop the empirical relationships covering a large CDOM range to convert all the CDOM absorption data in the literature to a fixed wavelength. Considering that $a(350)$ is widely used in the literature, we attempted to develop empirical relationships between $a(350)$ and $a(\lambda)$ for the other wavelengths. We compiled the available CDOM data covering different water clarity (Secchi disc depth ranging from 0.05 to 10.0 m) and trophic gradients (trophic state index ranging from 32.6 to 73.9) for inland waters in China (Fig. S3, Table S3). In addition, we also collected CDOM data in reservoir, lake, river from USA and the Netherland (Zhu et al., 2014) (Table S3). A large dataset of 766 samples with $a(350)$ from 0.14 to 19.55 m^{-1} covering >90% of the missing $a(350)$ ranges was obtained (Table S2). Based on this large dataset from various inland waters of different countries, we further developed empirical relationships between $a(350)$ and $a(254)$ ($r^2 = 96$, $p < 0.001$, Fig. 4a), $a(280)$ ($r^2 = 97$, $p < 0.001$, Fig. 4b), $a(300)$ ($r^2 = 99$, $p < 0.001$, Fig. 4c), $a(330)$ ($r^2 = 99$, $p < 0.001$, Fig. 4d), $a(375)$ ($r^2 = 99$, $p < 0.001$, Fig. 4e), and $a(440)$ ($r^2 = 83$, $p < 0.001$, Fig. 4f). All these correlations are highly significant and allowed us to convert all the literature CDOM absorption data to $a(350)$ with high precision (Fig. 4).

Consequently, a global $a(350)$ dataset was generated to demonstrate the CDOM distribution using the empirical relationship in Fig. 4 and all the available CDOM absorption data, including values ranging from <0.14 to higher than 20 m^{-1}, covering different inland waters such as lakes, rivers, reservoirs, ponds, and wetlands (Fig. 5). The dataset covering 791 waters revealed no significant correlation between latitude and $a(350)$, indicating that there is no latitudinal zonal distribution of CDOM and that decreasing temperature does not stimulate the accumulation of CDOM at the global scale. Exceptionally, clear alpine lakes show significant latitudinal trends that are imposed by dust deposition, flux of incident UVR, and bacterial processing (Mladenov et al., 2011). For complex inland waters, the spatial and temporal distributions of CDOM absorption are associated with sources and sinks from the perspective of human activities in the watersheds and the inherent properties of water bodies (Brezonik et al., 2015; Matthews, 2011). Therefore, it is understandable that there is no marked consistent global distribution of CDOM.

CDOM is derived from allochthonous and autochthonous sources. Specifically, allochthonous origins include inflow runoff, groundwater, atmospheric precipitation, and anthropogenic discharge of industrial

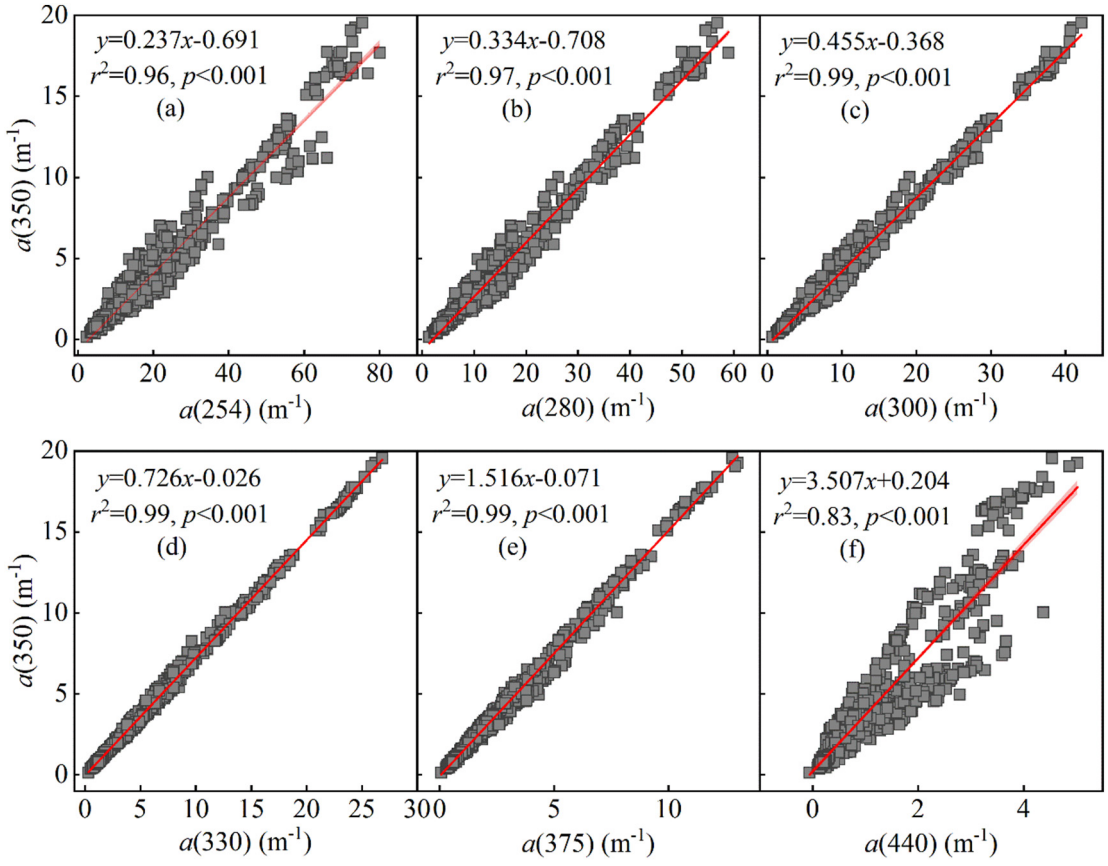

Fig. 4. Empirical relationships between $a(350)$ and $a(\lambda)$ of other wavelengths based on the dataset with CDOM samples collected from inland waters across China, USA and Netherland ($n = 766$).

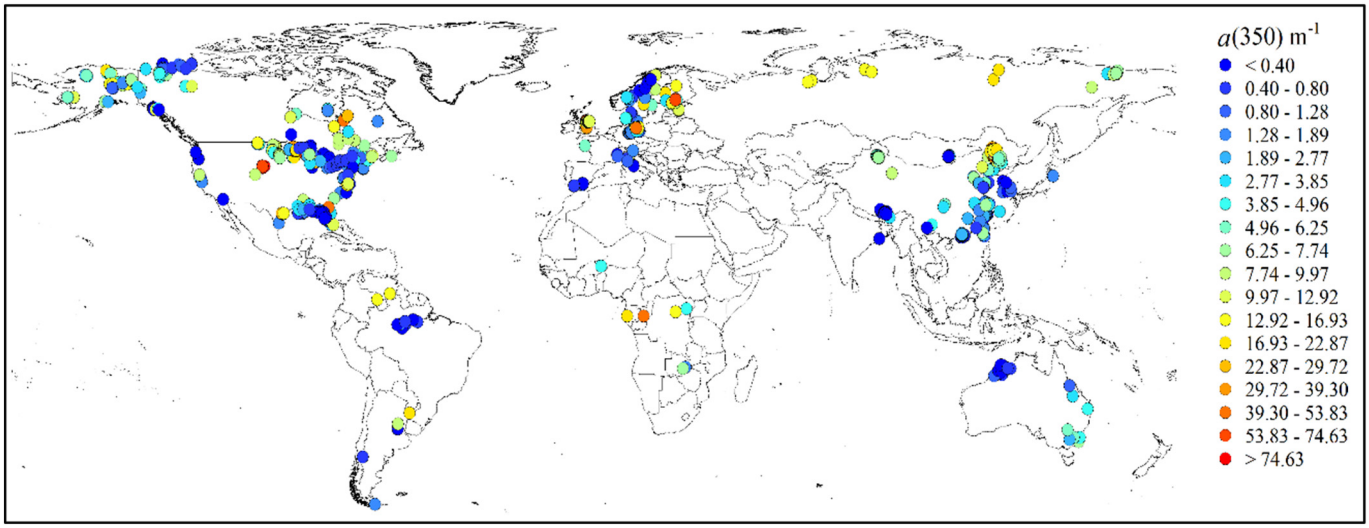

Fig. 5. Spatial distribution of the CDOM absorption coefficient in inland waters. The detailed dataset can be found in the Supporting Information (Table S2).

and domestic sewage. Autochthonous inputs are CDOM derived from microbial decomposition of phytoplankton and submerged plants, microbial production of extracellular polymeric substances, and pore water released from sediments (Fig. 6). For FDOM analysis, PARAFAC-derived humic-like components are categorized as allochthonous inputs, while protein-like components are often regarded as autochthonous microbial sources. Inland waters act as collectors, microcosms, and reactors that receive a mixture of allochthonous and autochthonous sources of CDOM (Tranvik et al., 2018), which are strongly influenced by natural processes and human activities and show high spatial heterogeneity, making it extremely difficult to accurately identify the CDOM sources and composition.

At regional and macroscopic scales, meteorological and hydrological processes and watershed-related factors, including soil type and land use – especially urban and agricultural land use upstream of the receiving water bodies, together with the inherent properties of water bodies, such as trophic status and ecosystem type, are often the key factors driving the changes in CDOM sources and composition in inland waters (Arvola et al., 2016; Zhang et al., 2018). Meteorological and hydrological processes such as climate warming, UVR, precipitation and inflow runoff from upstream watersheds change the CDOM sources and composition by impacting allochthonous and autochthonous inputs and the transformation of CDOM (Häder et al., 2007; Kellerman et al., 2014; Larsen et al., 2010; Mosley, 2015; Shi et al., 2020; Spencer et al., 2009). Therefore, any meteorological and hydrological processes induced by climate change will profoundly affect the CDOM sources and patterns in inland waters (Ejarque et al., 2018; Haaland et al., 2010; Häder et al., 2007; Mosley, 2015).

Previous studies have shown that the relative proportion and transformation of different land use types, including forests, grasslands, wetlands, agricultural land, and construction land, contribute to the variability in CDOM abundance, composition, and bioavailability in river and lake watersheds, as evidenced by a significant increase of terrestrial CDOM with increasing anthropogenic land use (cropland, urban construction) percentage (Arvola et al., 2016; Shi et al., 2020; Wilson and Xenopoulos, 2009). More specifically, forest coverage in an upstream watershed is positively correlated with the $SUVA_{254}$ value of downstream-linked waters, indicating that an increase in forest coverage can lead to enhanced input of humic-rich CDOM to lakes (Groeneveld et al., 2016; Williams et al., 2010). The structural

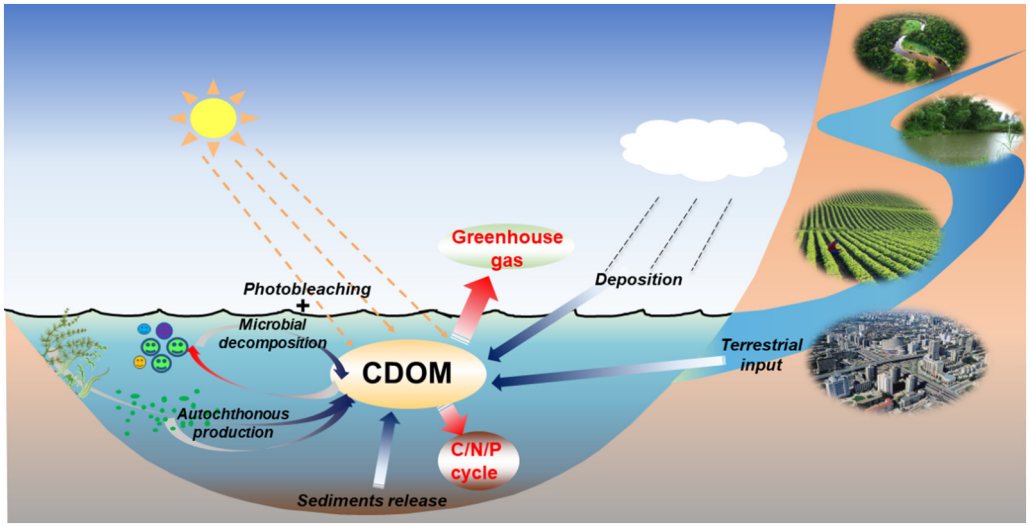

Fig. 6. Conceptual model of CDOM sources and transformation processes in aquatic ecosystems.

complexity of DOM decreases as the ratio of continuous croplands to wetlands increases (Wilson and Xenopoulos, 2009). Moreover, the trophic status might be used to determine whether a lake is a net source or sink of CDOM and DOC, while the water retention time along with the exchange cycle control the rate and flux of CDOM and DOC generation and consumption (Catalán et al., 2016; Evans et al., 2017; Kothawala et al., 2014). Specifically, oligotrophic lakes having low trophic status index are usually carbon sinks, and the degree of DOC mineralization increases significantly with prolonged water retention time, while eutrophic lakes corresponding to the high trophic status index are often carbon sources with notable correlation between the autochthonous-derived DOC concentration and the water retention time (Evans et al., 2017). For example, 74% of 57 oligotrophic waterbodies were net sinks, whereas 76% of 25 *meso*−/eutrophic waterbodies were net sources (44%) or balanced (32%) in 82 predominantly European and North American water bodies with varying nutrient concentrations (Evans et al., 2017).

At individual and micro scale, the physical, chemical, and biological processes occurring in inland waters, including water retention, stratification, photochemical degradation, and cyanobacterial blooms, drive the CDOM biogeochemical cycles in lakes. Water retention time, as an important index comprehensively reflecting CDOM sources, photodegradation, and microbial decomposition, has been widely used to trace the quantity and quality of CDOM (Evans et al., 2017; Kellerman et al., 2014; Kothawala et al., 2014; Lambert et al., 2016). In some highly eutrophic lakes, the microbial degradation of phytoplankton residues during algal blooms is a main contributor to the CDOM pool in water bodies (Zhang et al., 2009b). Additionally, for some urban lakes with serious air pollution and some remote alpine lakes, atmospheric dry and wet deposition is a crucial factor driving the changes in the CDOM amount, sources, and composition (Miller et al., 2009; Mladenov et al., 2011; Zhang et al., 2014). CDOM in lakes located below the treeline is strongly influenced by catchment vegetation and land use. In contrast, the atmospheric inputs of organic matter have greater effects on the CDOM amount and quality than inputs from terrestrial vegetation in the clear alpine lakes above treeline and (Ant)Arctic lakes located in barren catchments or catchments with poorly developed soils and vegetation (Mladenov et al., 2011).

CDOM dynamics in inland waters depend first and foremost on the magnitude, sources, and composition of both allochthonous inputs and autochthonous production. The balance between these different pathways ultimately determines the magnitude and transformation of CDOM in inland waters, which is largely influenced by the regulation of CDOM inputs and water residence times *via* hydrology, the impact to CDOM production by trophic state, the regulation of CDOM photodegradation by light attenuation, and control of microbial decomposition by water temperature. Therefore, more attention should be paid to climate-induced meteorological and hydrological processes to elucidate CDOM cycle processes and driving mechanisms in inland waters. In addition, the factors and driving mechanisms regulating CDOM dynamics in inland waters are complex and variable at different temporal and spatial scales. Therefore, it is difficult to clarify the specific processes that affect CDOM dynamics based on the analysis of samples collected from natural environments. Laboratory control experiments, larger scale controlled mesocosm and whole-lake experiments can help identify the effects of specific factors on CDOM dynamics. The design of comprehensive experiments considering the concurrent effects is encouraged to elucidate the processes and mechanisms that affect CDOM dynamics in inland waters.

Analytical approaches, observation data, and cycle processes could be coupled to develop numerical models to acquire more detailed understanding and important insights of CDOM dynamics and climate feedbacks in inland waters. Modeling approaches can be performed at different scales: (1) large watershed scale, (2) mesoscale ecosystem scale, and (3) microcosmic production and degradation scale. At the large watershed scale, the developed models are based on a combination of hydrological and biogeochemical processes to simulate the input and transformation of CDOM from the watershed to water. At the mesoscale ecosystem scale, the models are used to simulate the vertical and horizontal dynamics of CDOM and the related phytoplankton, zooplankton biomass, nutrients, *etc.* At the microcosmic scale, the models focus on CDOM production, photodegradation and microbial decomposition, which is highly supported by laboratory and microcosm experiments. All these models require substantial field and laboratory data, including hydrological, physical, chemical, and ecological data, collaborative and interdisciplinary work with analytical chemists, hydrologists, limnologists, ecologists, remote sensing scientists and modelers.

6. Mechanisms of CDOM transformation and environmental effects

CDOM transformation is largely influenced by both photochemical and microbial processes (Fig. 6). Numerous field and laboratory studies have confirmed that CDOM undergoes significant photochemical reactions and cleavage of chemical bonds after absorbing UVR, causing decreasing absorption and fluorescence (Aulló-Maestro et al., 2017; Loiselle et al., 2012; Zhang et al., 2009a). For example, a photobleaching experiment involving 7 days' exposure to natural UVR resulted in a marked decrease in allochthonous CDOM absorption (7.04 to 3.36 m^{-1}, 42% decrease) in a large shallow temperate lake (Aulló-Maestro et al., 2017). Meanwhile, the composition and molecular weight of CDOM will change as well, as evidenced by significantly increasing values of $S_{275–295}$ and S_R, which indicates a decreased molecular weight of CDOM (Aulló-Maestro et al., 2017; Helms et al., 2008; Osburn et al., 2011; Zhang et al., 2013a). Previous studies have also shown that humic-like CDOM is more easily degraded by light, while protein-like substances can resist photodegradation and persist in water bodies (Aulló-Maestro et al., 2017; Kellerman et al., 2015; Zhang et al., 2013b; Zhang et al., 2009b). In addition, photochemical alteration of CDOM will also affect the forms, distribution, transformation, and subsequent toxicity and bioavailability for binding heavy metals and organic pollutants (Shiu and Lee, 2017; Yan et al., 2013).

Reactions with reactive oxygen species (ROS) including singlet oxygen and superoxide generated during irradiation, being an important phototransformation mechanism, play a vital role in the transformation of CDOM due to the high photochemical activity and apparent quantum yield (Cory et al., 2010; Scully et al., 2003; Waggoner et al., 2017). Nevertheless, phototransformation of CDOM reduces its ability to further generate ROS due to decreased light absorption. Thus, the role of ROS in the long term and persistent photoactivity of CDOM still need/require further investigation.

Microbial decomposition is another path of the CDOM cycle in inland waters. Microbial decomposition may not only significantly reduce CDOM absorption and DOC concentrations but also notably change the composition and structure of CDOM (Wachenfeldt et al., 2009; Williams et al., 2010; Zhou et al., 2019). The degree of degradation by microbes cultured for 500 days under dark conditions was similar to that under photodegradation for 7 days, indicating a much higher photodegradation efficiency of microbes than of microorganisms under experimental conditions (Cory and Kling, 2018; Vähätalo and Wetzel, 2004). However, photodegradation mainly occurs in surface water and on sunny days (Koehler et al., 2014), while microbial degradation occurs ubiquitously. Therefore, it is difficult to determine the relative importance of microbes under field conditions, and photodegradation and microbial decomposition often complement and promote each other, as previously revealed by significant improvements in the bioavailability and transformation efficiency of CDOM after photodegradation (Piccini et al., 2009; Sankar et al., 2019; Su et al., 2017). Overall, the combined effects of light and bacteria are more efficient than the individual effects of light or bacteria in remineralizing and altering CDOM (Madsen-Østerbye et al., 2018). Another study demonstrated that photodegradation together with microbial decomposition could completely mineralize at least some forms of wetland-derived

DOM, even biologically recalcitrant allochthonous DOM, in surface waters with sufficiently long residence times (Vähätalo and Wetzel, 2008). Consequently, the concentration and composition of CDOM in the surface water largely depend on the dynamic balance between various sources driven by meteorological and hydrological processes and transformations imposed by light and microbes.

Photodegradation and microbial decomposition of CDOM result in decreased DOC concentrations, absorption coefficients, and fluorescence intensities, changes in molecular composition, as well as transformation of some of organic substances to inorganic components. Other abiotic processes transforming DOM may include self-assembly (Kerner et al., 2003; Xu and Guo, 2018) and autoxidative degradation (Galeron et al., 2018; Rontani et al., 2017). An incubation experiment revealed that carbohydrates and protein-like substances, especially the high molecular weight components, were overall preferentially decomposed by microorganisms, while the dynamic variations of the humic- and fulvic-like CDOM components was largely determined by the self-assembly (Xu and Guo, 2018). These processes jointly transform labile CDOM into refractory CDOM persistent in inland waters, and are accompanied by at least three environmental effects.

1) They affect the underwater light, especially UVR attenuation. Many studies have demonstrated that UVR, including UV-B and UV-A radiation diffuse attenuation coefficients, were significantly correlated with CDOM absorption coefficients (Gareis et al., 2010; Laurion et al., 2000; Morris et al., 1995). Therefore, any processes resulting in changes in total CDOM abundance, sources, or composition will alter UVR attenuation and underwater UVR exposure. Specific reasons include climate warming, permafrost melting, changing precipitation induced by climate change, increasing land use change caused by intense human activities, increasing dust inputs, and changing photodegradation and microbial decomposition (Kellerman et al., 2014; Kothawala et al., 2014; Mladenov et al., 2011; Wilson and Xenopoulos, 2009). For example, long-term lake browning due to increases in CDOM was reported to significantly increase UVR attenuation (Williamson et al., 2015; Wolf and Heuschele, 2018). In contrast, photobleaching, resulting in decreased CDOM absorption and fluorescence intensity, decreased UVR attenuation and increased euphotic zone depths in the water column, thereby further affecting the structure and function of aquatic ecosystems. This impact is especially pronounced in alpine clear water lakes at high altitudes with strong UVR (Clements et al., 2008; Sulzberger and Durisch-Kaiser, 2009; Williamson et al., 2014).

2) They alter polymer compounds. Photodegradation and microbial decomposition result in conversion of CDOM that are not readily assimilated by organisms into low-molecular-weight organic compounds, along with the release of soluble reactive phosphorus, soluble inorganic nitrogen, nitrite, ammonia and a number of other inorganic nutrients. This process accelerates nutrient circulation and regeneration in the water column and thereby supports the growth of microbes and phytoplankton by providing carbon, nitrogen, phosphorus, and other biogenic elements (Bastidas Navarro and Modenutti, 2010; Jeff et al., 2012; Mesfioui et al., 2015; Su et al., 2017). The exposure of CDOM to UVR causes rapid changes in bacterial activity and community composition due to increased bioavailability of simple organic substrates after CDOM exposure to UVR (Piccini et al., 2009). For the nitrogen cycle of CDOM, release of ammonium *via* photoammonification is an important pathway and mechanism (Jeff et al., 2012; Stedmon et al., 2007). However, the driving mechanism of phosphorus mineralization from CDOM is yet unclear.

3) They promote greenhouse gas emissions. A large amount of greenhouse gases, such as carbon dioxide (CO_2), methane (CH_4), carbon monoxide (CO), and carbonyl sulfide (COS), is released during the process of CDOM mineralization, ultimately exacerbating global warming (Lapierre et al., 2013; Rasilo et al., 2015; Williamson et al., 2014; Zhang and Xie, 2015). A large-scale study of 224 lakes covering a wide range of lake types and environmental gradients in Québec showed that increasing CDOM concentrations led to increased CO_2 flux but decreased CH_4 flux (Rasilo et al., 2015). Quantitative analysis conducted in extensive lake investigations in Sweden showed that direct photochemical mineralization of CDOM contributed 1–12% of the total CO_2 emissions, exhibiting large differentiation (Groeneveld et al., 2016; Koehler et al., 2014). In addition, the indirect effects of a stimulated microbial respiration corroborates the notion that microbial decomposition in a warming climate will contribute substantially to greenhouse gas emissions in inland waters (Koehler et al., 2014), which in turn will exacerbate global warming. However, the actual contribution and driving mechanism of CDOM to overall CO_2 and CH_4 emissions in inland waters remains largely speculative. We still lack deep understanding and global estimates of greenhouse gas emissions from CDOM in inland waters, meaning that more field, experimental, and model work is required to improve our understanding of the underlying mechanisms driving different greenhouse gas productions and the role of CDOM in global warming.

7. Conclusions

The past 30 years have seen rapid developments in various types of techniques and methods for characterizing the abundance, sources, and composition of CDOM, contributing to an improved understanding of the CDOM distribution, cycle, and transformation. Optical, isotope, and mass spectrometric techniques are used to characterize CDOM abundance, composition, and sources, and remote sensing and high frequency observation can map CDOM distribution with high temporal and spatial resolutions. CDOM dynamics are mainly determined by watershed-related processes and biogeochemical cycling. The photochemical degradation and microbial decomposition are the underlying mechanisms of CDOM cycle. Our review provides an interdisciplinary view and new insights on CDOM dynamics in inland waters. However, more work is clearly needed on the characterization, tracing, and dynamics of CDOM, which is substantially challenged by the high complexity, heterogeneity, and rapid variation and turnover of CDOM in inland waters.

Declaration of competing interest

The authors declare that they have no conflicts of interest.

Acknowledgments

This study was jointly funded by the National Natural Science Foundation of China (grants 41930760, 41621002, 41771514, and 41807362) and Water Resource Science and Technology Project in Jiangsu Province (2020057). EJ was supported by the TÜBITAK, BIDEB 2232 program (118C250). We would like to thank Kanshan Song and Stefan Simis for their CDOM data in USA and Netherland. We would like to express our gratitude to the four anonymous reviewers and the associate editor for their critical and constructive comments.

Appendix A. Supplementary data

Supplementary data to this article can be found online at https://doi.org/10.1016/j.scitotenv.2020.143550.

References

Al-Kharusi, E.S., Tenenbaum, D.E., Abdi, A.M., Kutser, T., Karlsson, J., Bergstrom, A.K., Berggren, M., 2020. Large-scale retrieval of coloured dissolved organic matter in northern lakes using Sentinel-2 data. Remote Sens. 12 (1).

Arvola, L., Äijälä, C., Leppäranta, M., 2016. CDOM concentrations of large Finnish lakes relative to their landscape properties. Hydrobiologia 780 (1), 37–46.

Aulló-Maestro, M.E., Hunter, P., Spyrakos, E., Mercatoris, P., Kovacs, A.W., Horváth, H., Preston, T., Présing, M., Torres Palenzuela, J.M., Tyler, A., 2017. Spatio-seasonal variability of chromophoric dissolved organic matter absorption and responses to photobleaching in a large shallow temperate lake. Biogeosciences 14, 1215–1233.

Bastidas Navarro, M., Modenutti, B., 2010. UVR induce optical changes and phosphorous release of lake water and macrophyte leachates in shallow Andean lakes. J. Limnol. 69 (1), 112–119.
Battin, T.J., Luyssaert, S., Kaplan, L.A., Aufdenkampe, A.K., Richter, A., Tranvik, L.J., 2009. The boundless carbon cycle. Nat. Geosci. 2 (9), 598–600.
Brezonik, P.L., Olmanson, L.G., Finlay, J.C., Bauer, M.E., 2015. Factors affecting the measurement of CDOM by remote sensing of optically complex inland waters. Remote Sens. Environ. 157, 199–215.
Cao, F., Miller, W.L., 2015. A new algorithm to retrieve chromophoric dissolved organic matter (CDOM) absorption spectra in the UV from ocean color. J. Geophys. Res. Oceans 120 (1), 496–516.
Cao, F., Tzortziou, M., Hu, C.M., Mannino, A., Fichot, C.G., Del Vecchio, R., Najjar, R.G., Novak, M., 2018. Remote sensing retrievals of colored dissolved organic matter and dissolved organic carbon dynamics in north American estuaries and their margins. Remote Sens. Environ. 205, 151–165.
Catalán, N., Marcé, R., Kothawala, D.N., Tranvik, L.J., 2016. Organic carbon decomposition rates controlled by water retention time across inland waters. Nat. Geosci. 9 (7), 501–504.
Chen, W., Westerhoff, P., Leenheer, J.A., Booksh, K., 2003. Fluorescence excitation-emission matrix regional integration to quantify spectra for dissolved organic matter. Environ. Sci. Technol. 37 (24), 5701–5710.
Chen, W., Teng, C.-Y., Qian, C., Yu, H.-Q., 2019a. Characterizing properties and environmental behaviors of dissolved organic matter using two-dimensional correlation spectroscopic analysis. Environ. Sci. Technol. 53 (9), 4683–4694.
Chen, Y., Arnold, W.A., Griffin, C.G., Olmanson, L.G., Brezonik, P.L., Hozalski, R.M., 2019b. Assessment of the chlorine demand and disinfection byproduct formation potential of surface waters via satellite remote sensing. Water Res. 165, 115001.
Clements, W.H., Brooks, M.L., Kashian, D.R., Zuellig, R.E., 2008. Changes in dissolved organic material determine exposure of stream benthic communities to UV-B radiation and heavy metals: implications for climate change. Glob. Chang. Biol. 14 (9), 2201–2214.
Coble, P.G., 1996. Characterization of marine and terrestrial DOM in seawater using excitation emission matrix spectroscopy. Mar. Chem. 51 (4), 325–346.
Cory, R.M., Kling, G.W., 2018. Interactions between sunlight and microorganisms influence dissolved organic matter degradation along the aquatic continuum: interactions between sunlight and microorganisms. Limnology and Oceanography Letters 3 (3), 102–116.
Cory, R.M., McNeill, K., Cotner, J.P., Amado, A., Purcell, J.M., Marshall, A.G., 2010. Singlet oxygen in the coupled photochemical and biochemical oxidation of dissolved organic matter. Environ. Sci. Technol. 44 (10), 3683–3689.
Coward, E.K., Ohno, T., Sparks, D.L., 2019. Direct evidence for temporal molecular fractionation of dissolved organic matter at the iron oxyhydroxide interface. Environ. Sci. Technol. 53 (2), 642–650.
Cuss, C.W., Gueguen, C., 2015. Relationships between molecular weight and fluorescence properties for size-fractionated dissolved organic matter from fresh and aged sources. Water Res. 68, 487–497.
De Haan, H., De Boer, T., 1987. Applicability of light absorbance and fluorescence as measures of concentration and molecular size of dissolved organic carbon in humic Lake Tjeukemeer. Water Res. 21 (6), 731–734.
Dierssen, H.M., 2010. Perspectives on empirical approaches for ocean color remote sensing of chlorophyll in a changing climate. Proc. Natl. Acad. Sci. U. S. A. 107 (40), 17073–17078.
Dittmar, T., Stubbins, A., 2014. Dissolved organic matter in aquatic systems. In: Holland, H.D., Turekian, K.K. (Eds.), Treatise on Geochemistry, 2nd edition Elsevier Ltd, pp. 125–156.
Dittmar, T., Koch, B., Hertkorn, N., Kattner, G., 2008. A simple and efficient method for the solid-phase extraction of dissolved organic matter (SPE-DOM) from seawater. Limnology and Oceanography-Methods 6, 230–235.
Dittmar, T., De Rezende, C.E., Manecki, M., Niggemann, J., Ovalle, A.R.C., Stubbins, A., Bernardes, M.C., 2012. Continuous flux of dissolved black carbon from a vanished tropical forest biome. Nat. Geosci. 5 (9), 618–622.
Downing, J., Prairie, Y., Cole, J., Duarte, C., Tranvik, L., Striegl, R., McDowell, W., Kortelainen, P., Caraco, N., Melack, J., 2006. The global abundance and size distribution of lakes, ponds, and impoundments. Limnol. Oceanogr. 51 (5), 2388–2397.
Drake, T.W., Raymond, P.A., Spencer, R.G., 2018. Terrestrial carbon inputs to inland waters: a current synthesis of estimates and uncertainty. Limnology and Oceanography Letters 3 (3), 132–142.
Ejarque, E., Khan, S., Steniczka, G., Schelker, J., Kainz, M.J., Battin, T.J., 2018. Climate-induced hydrological variation controls the transformation of dissolved organic matter in a subalpine lake. Limnol. Oceanogr. 63 (3), 1355–1371.
Emilson, E.J., Carson, M.A., Yakimovich, K.M., Osterholz, H., Dittmar, T., Gunn, J., Mykytczuk, N., Basiliko, N., Tanentzap, A.J., 2018. Climate-driven shifts in sediment chemistry enhance methane production in northern lakes. Nat. Commun. 9 (1), 1801.
Evans, C.D., Futter, M.N., Moldan, F., Valinia, S., Frogbrook, Z., Kothawala, D.N., 2017. Variability in organic carbon reactivity across lake residence time and trophic gradients. Nat. Geosci. 10 (11), 832–835.
Ficek, D., Zapadka, T., Dera, J., 2011. Remote sensing reflectance of Pomeranian lakes and the Baltic. Oceanologia 53 (4), 959–970.
Galeron, M.A., Radakovitch, O., Charriere, B., Vaultier, F., Volkman, J.K., Bianchi, T.S., Ward, N.D., Medeiros, P.M., Sawakuchi, H.O., Tank, S., Kerherve, P., Rontani, J.F., 2018. Lipoxygenase-induced autoxidative degradation of terrestrial particulate organic matter in estuaries: a widespread process enhanced at high and low latitude. Org. Geochem. 115, 78–92.
Gareis, J.A.L., Lesack, L.F.W., Bothwell, M.L., 2010. Attenuation of *in situ* UV radiation in Mackenzie Delta lakes with varying dissolved organic matter compositions. Water Resour. Res. 46 (9), 2095–2170.
Gitelson, A.A., Schalles, J.F., Hladik, C.M., 2007. Remote chlorophyll-a retrieval in turbid, productive estuaries: Chesapeake Bay case study. Remote Sens. Environ. 109, 464–472.
Glibert, P.M., Middelburg, J.J., McClelland, J.W., Zanden, M.J.V., 2019. Stable isotope tracers: enriching our perspectives and questions on sources, fates, rates, and pathways of major elements in aquatic systems. Limnol. Oceanogr. 64 (3), 950–981.
Goldberg, S., Ball, G., Allen, B., Schladow, S., Simpson, A., Masoom, H., Soong, R., Graven, H., Aluwihare, L., 2015. Refractory dissolved organic nitrogen accumulation in high-elevation lakes. Nat. Commun. 6, 6347.
Griffin, C.G., Frey, K.E., Rogan, J., Holmes, R.M., 2011. Spatial and interannual variability of dissolved organic matter in the Kolyma River, East Siberia, observed using satellite imagery. J. Geophys. Res. Biogeosci. 116 (G3).
Griffin, C.G., Finlay, J.C., Brezonik, P.L., Leif, O., Hozalski, R.M., 2018. Limitations on using CDOM as a proxy for DOC in temperate lakes. Water Res. 144, 719–727.
Groeneveld, M., Tranvik, L., Natchimuthu, S., Koehler, B., 2016. Photochemical mineralisation in a boreal brown water lake: considerable temporal variability and minor contribution to carbon dioxide production. Biogeosciences 13 (13), 3931–3943.
Haaland, S., Hongve, D., Laudon, H., Riise, G., Vogt, R., 2010. Quantifying the drivers of the increasing colored organic matter in boreal surface waters. Environ. Sci. Technol. 44 (8), 2975–2980.
Häder, D.P., Kumar, H.D., Smith, R.C., Worrest, R.C., 2007. Effects of solar UV radiation on aquatic ecosystems and interactions with climate change. Photochem. Photobiol. Sci. 6 (3), 267–285.
Hansell, D.A., Carlson, C.A., 2015. Biogeochemistry of Marine Dissolved Organic Matter. Second edition. Academic Press (1-667 pp).
Helms, J.R., Stubbins, A., Ritchie, J.D., Minor, E.C., Kieber, D.J., Mopper, K., 2008. Absorption spectral slopes and slope ratios as indicators of molecular weight, source, and photobleaching of chromophoric dissolved organic matter. Limnol. Oceanogr. 53 (3), 955–969.
Hood, E., Fellman, J., Spencer, R.G., Hernes, P.J., Edwards, R., D'Amore, D., Scott, D., 2009. Glaciers as a source of ancient and labile organic matter to the marine environment. Nature 462 (7276), 1044–1047.
Huguet, A., Vacher, L., Relexans, S., Saubusse, S., Froidefond, J.M., Parlanti, E., 2009. Properties of fluorescent dissolved organic matter in the Gironde estuary. Org. Geochem. 40 (6), 706–719.
Huovinen, P., Penttilä, H., Soimasuo, M., 2003. Spectral attenuation of solar ultraviolet radiation in humic lakes in Central Finland. Chemosphere 51 (3), 205–214.
Ike, I.A., Karanfil, T., Cho, J., Hur, J., 2019. Oxidation byproducts from the degradation of dissolved organic matter by advanced oxidation processes–a critical review. Water Res., 114929
Ishii, S.K., Boyer, T.H., 2012. Behavior of reoccurring PARAFAC components in fluorescent dissolved organic matter in natural and engineered systems: a critical review. Environ. Sci. Technol. 46 (4), 2006–2017.
Jeff, S., Hunter, K., Vandergucht, D., Hudson, J., 2012. Photochemical mineralization of dissolved organic nitrogen to ammonia in prairie lakes. Hydrobiologia 693 (1), 71–80.
Joshi, I.D., D'Sa, E.J., Osburn, C.L., Bianchi, T.S., Ko, D.S., Oviedo-Vargas, D., Arellano, A.R., Ward, N.D., 2017. Assessing chromophoric dissolved organic matter (CDOM) distribution, stocks, and fluxes in Apalachicola Bay using combined field, VIIRS Ocean color, and model observations. Remote Sens. Environ. 191, 359–372.
Juhls, B., Overduin, P.P., Holemann, J., Hieronymi, M., Matsuoka, A., Heim, B., Fischer, J., 2019. Dissolved organic matter at the fluvial-marine transition in the Laptev Sea using *in situ* data and ocean colour remote sensing. Biogeosciences 16 (13), 2693–2713.
Keith, D.J., Yoder, J.A., Freeman, S.A., 2002. Spatial and temporal distribution of coloured dissolved organic matter (CDOM) in Narragansett Bay, Rhode Island: implications for phytoplankton in coastal waters. Estuar. Coast. Shelf Sci. 55 (5), 705–717.
Kellerman, A.M., Dittmar, T., Kothawala, D.N., Tranvik, L.J., 2014. Chemodiversity of dissolved organic matter in lakes driven by climate and hydrology. Nat. Commun. 5, 3804.
Kellerman, A.M., Kothawala, D.N., Dittmar, T., Tranvik, L.J., 2015. Persistence of dissolved organic matter in lakes related to its molecular characteristics. Nat. Geosci. 8 (6), 454–457.
Kellerman, A.M., Arellano, A., Podgorski, D.C., Martin, E.E., Martin, J.B., Deuerling, K.M., Bianchi, T.S., Spencer, R.G.M., 2020. Fundamental drivers of dissolved organic matter composition across an Arctic effective precipitation gradient. Limnol. Oceanogr. 65 (6), 1217–1234.
Kerner, M., Hohenberg, H., Ertl, S., Reckermann, M., Spitzy, A., 2003. Self-organization of dissolved organic matter to micelle-like microparticles in river water. Nature 422 (6928), 150–154.
Koehler, B., Landelius, T., Weyhenmeyer, G.A., Machida, N., Tranvik, L.J., 2014. Sunlight-induced carbon dioxide emissions from inland waters. Glob. Biogeochem. Cycles 28 (7), 696–711.
Kothawala, D.N., Stedmon, C.A., Müller, R.A., Weyhenmeyer, G.A., Köhler, S.J., Tranvik, L.J., 2014. Controls of dissolved organic matter quality: evidence from a large-scale boreal lake survey. Glob. Chang. Biol. 20 (4), 1101–1114.
Kutser, T., 2012. The possibility of using the Landsat image archive for monitoring long time trends in coloured dissolved organic matter concentration in lake waters. Remote Sens. Environ. 123 (3), 334–338.
Kutser, T., Pierson, D.C., Kallio, K.Y., Reinart, A., Sobek, S., 2005. Mapping lake CDOM by satellite remote sensing. Remote Sens. Environ. 94 (4), 535–540.
Lambert, T., Teodoru, C.R., Nyoni, F.C., Bouillon, S., Darchambeau, F., Massicotte, P., Borges, A.V., 2016. Along-stream transport and transformation of dissolved organic matter in a large tropical river. Biogeosciences 13 (9), 2727–2741.

Lapierre, J.F., Guillemette, F., Berggren, M., del Giorgio, P.A., 2013. Increases in terrestrially derived carbon stimulate organic carbon processing and CO_2 emissions in boreal aquatic ecosystems. Nat. Commun. 4 (1), 2972.
Larsen, L.G., Aiken, G.R., Harvey, J.W., Noe, G.B., Crimaldi, J.P., 2010. Using fluorescence spectroscopy to trace seasonal DOM dynamics, disturbance effects, and hydrologic transport in the Florida Everglades. J. Geophys. Res. 115 (G3).
Laurion, I., Ventura, M., Catalan, J., Psenner, R., Sommaruga, R., 2000. Attenuation of ultraviolet radiation in mountain lakes: factors controlling the among-and within-lake variability. Limnol. Oceanogr. 45 (6), 1274–1288.
Lavonen, E.E., Kothawala, D.N., Tranvik, L.J., Gonsior, M., Schmitt-Kopplin, P., Köhler, S.J., 2015. Tracking changes in the optical properties and molecular composition of dissolved organic matter during drinking water production. Water Res. 85, 286–294.
Lee, M.-H., Lee, Y.K., Derrien, M., Choi, K., Shin, K.H., Jang, K.-S., Hur, J., 2019. Evaluating the contributions of different organic matter sources to urban river water during a storm event via optical indices and molecular composition. Water Res. 165, 115006.
Li, P., Hur, J., 2017. Utilization of UV-vis spectroscopy and related data analyses for dissolved organic matter (DOM) studies: a review. Crit. Rev. Environ. Sci. Technol. 47 (3), 131–154.
Li, J., Yu, Q., Tian, Y.Q., Becker, B.L., 2017. Remote sensing estimation of colored dissolved organic matter (CDOM) in optically shallow waters. ISPRS J. Photogramm. Remote Sens. 128, 98–110.
Li, J., Yu, Q., Tian, Y.Q., Becker, B.L., Siqueira, P., Torbick, N., 2018. Spatio-temporal variations of CDOM in shallow inland waters from a semi-analytical inversion of Landsat-8. Remote Sens. Environ. 218, 189–200.
Loiselle, S., Vione, D., Minero, C., Maurino, V., Tognazzi, A., Dattilo, A.M., Rossi, C., Bracchini, L., 2012. Chemical and optical phototransformation of dissolved organic matter. Water Res. 46 (10), 3197–3207.
Madsen-Østerbye, M., Kragh, T., Pedersen, O., Sand-Jensen, K., 2018. Coupled UV-exposure and microbial decomposition improves measures of organic matter degradation and light models in humic lake. Ecol. Eng. 118, 191–200.
Mannino, A., Russ, M.E., Hooker, S.B., 2008. Algorithm development and validation for satellite-derived distributions of DOC and CDOM in the US middle Atlantic bight. Journal of Geophysical Research: Oceans (1978–2012) 113 (C7).
Maritorena, S., Siegel, D.A., Peterson, A.R., 2002. Optimization of a semianalytical ocean color model for global-scale applications. Appl. Opt. 41 (15), 2705–2714.
Massicotte, P., Asmala, E., Stedmon, C., Markager, S., 2017. Global distribution of dissolved organic matter along the aquatic continuum: across rivers, lakes and oceans. Sci. Total Environ. 609, 180–191.
de Matos Valerio, A., Kampel, M., Vantrepotte, V., Ward, N.D., Sawakuchi, H.O., Less, D.F.D.S., Neu, V., Cunha, A., Richey, J., 2018. Using CDOM optical properties for estimating DOC concentrations and pCO 2 in the lower Amazon River. Opt. Express 26 (14), A657–A677.
Matthews, M.W., 2011. A current review of empirical procedures of remote sensing in inland and near-coastal transitional waters. Int. J. Remote Sens. 32 (21), 6855–6899.
McKnight, D.M., Boyer, E.W., Westerhoff, P.K., Doran, P.T., Kulbe, T., Andersen, D.T., 2001. Spectrofluorometric characterization of dissolved organic matter for indication of precursor organic material and aromaticity. Limnol. Oceanogr. 46 (1), 38–48.
Menken, K.D., Brezonik, P.L., Bauer, M.E., 2006. Influence of chlorophyll and colored dissolved organic matter (CDOM) on lake reflectance spectra: implications for measuring lake properties by remote sensing. Lake and Reservoir Management 22 (3), 179–190.
Mesfioui, R., Abdulla, H.A., Hatcher, P.G., 2015. Photochemical alterations of natural and anthropogenic dissolved organic nitrogen in the York River. Environ. Sci. Technol. 49 (1), 159–167.
Miao, S., Lyu, H., Wang, Q., Li, Y., Wu, Z., Du, C., Bi, S., Mu, M., Lei, S., 2019. Estimation of terrestrial humic-like substances in inland lakes based on the optical and fluorescence characteristics of chromophoric dissolved organic matter (CDOM) using OLCI images. Ecol. Indic. 101, 399–409.
Mihalevich, B.A., Horsburgh, J.S., Melcher, A.A., 2017. High-frequency measurements reveal spatial and temporal patterns of dissolved organic matter in an urban water conveyance. Environ. Monit. Assess. 189 (11), 593.
Miller, C., Gordon, K.G., Kieber, R.J., Willey, J.D., Seaton, P.J., 2009. Chemical characteristics of chromophoric dissolved organic matter in rainwater. Atmos. Environ. 43 (15), 2497–2502.
Mladenov, N., Sommaruga, R., Moralesbaquero, R., Laurion, I., Camarero, L., Diéguez, M.C., Camacho, A., Delgado, A., Torres, O., Chen, Z., 2011. Dust inputs and bacteria influence dissolved organic matter in clear alpine lakes. Nat. Commun. 2 (3), 405.
Mopper, K., Stubbins, A., Ritchie, J.D., Bialk, H.M., Hatcher, P.G., 2007. Advanced instrumental approaches for characterization of marine dissolved organic matter: extraction techniques, mass spectrometry, and nuclear magnetic resonance spectroscopy. Chem. Rev. 107 (2), 419–442.
Morris, D.P., Zagarese, H., Williamson, C.E., Balseiro, E.G., Hargreaves, B.R., Modenutti, B., Moeller, R., Queimalinos, C., 1995. The attenuation of solar UV radiation in lakes and the role of dissolved organic carbon. Limnol. Oceanogr. 40 (8), 1381–1391.
Mosley, L.M., 2015. Drought impacts on the water quality of freshwater systems; review and integration. Earth Sci. Rev. 140, 203–214.
Murphy, K.R., Stedmon, C.A., Graeber, D., Bro, R., 2013. Fluorescence spectroscopy and multi-way techniques. PARAFAC. Anal. Methods 5 (23), 6557–6566.
Murphy, K.R., Timko, S.A., Gonsior, M., Powers, L.C., Wunsch, U.J., Stedmon, C.A., 2018. Photochemistry illuminates ubiquitous organic matter fluorescence spectra. Environ. Sci. Technol. 52 (19), 11243–11250.
Nebbioso, A., Piccolo, A., 2013. Molecular characterization of dissolved organic matter (DOM): a critical review. Anal. Bioanal. Chem. 405 (1), 109–124.
Nelson, N.B., Siegel, D.A., 2013. The global distribution and dynamics of chromophoric dissolved organic matter. Annu. Rev. Mar. Sci. 5, 447–476.
Odermatt, D., Gitelson, A., Brando, V.E., Schaepman, M., 2012. Review of constituent retrieval in optically deep and complex waters from satellite imagery. Remote Sens. Environ. 118, 116–126.
Ohno, T., Parr, T.B., Gruselle, M.C.c.I., Fernandez, I.J., Sleighter, R.L., Hatcher, P.G., 2014. Molecular composition and biodegradability of soil organic matter: a case study comparing two New England forest types. Environ. Sci. Technol. 48 (13), 7229–7236.
Olmanson, L.G., Brezonik, P.L., Finlay, J.C., Bauer, M.E., 2016. Comparison of Landsat 8 and Landsat 7 for regional measurements of CDOM and water clarity in lakes. Remote Sens. Environ. 185, 119–128.
Osburn, C.L., Wigdahl, C.R., Fritz, S.C., Saros, J.E., 2011. Dissolved organic matter composition and photoreactivity in prairie lakes of the U.S. Great Plains. Limnol. Oceanogr. 56 (6), 2371–2390.
Perdue, E.M., Ritchie, J.D., 2003. Dissolved organic matter in freshwaters. In: Holland, H.D., Turekian, K.K. (Eds.), Treatise on Geochemistry. Elsevier Ltd, pp. 273–318.
Piccini, C., Conde, D., Pernthaler, J., Sommaruga, R., 2009. Alteration of chromophoric dissolved organic matter by solar UV radiation causes rapid changes in bacterial community composition. Photochem. Photobiol. Sci. 8 (9), 1321–1328.
Rasilo, T., Prairie, Y.T., Giorgio, P.A., 2015. Large-scale patterns in summer diffusive CH4 fluxes across boreal lakes, and contribution to diffusive C emissions. Glob. Chang. Biol. 21 (3), 1124–1139.
Raymond, P.A., Bauer, J.E., 2001. Riverine export of aged terrestrial organic matter to the North Atlantic Ocean. Nature 409 (6819), 497–500.
Riedel, T., Dittmar, T., 2014. A method detection limit for the analysis of natural organic matter via Fourier transform ion cyclotron resonance mass spectrometry. Anal. Chem. 86 (16), 8376–8382.
Romera-Castillo, C., Chen, M.L., Yamashita, Y., Jaffe, R., 2014. Fluorescence characteristics of size-fractionated dissolved organic matter: implications for a molecular assembly based structure? Water Res. 55, 40–51.
Rontani, J.F., Galeron, M.A., Amiraux, R., Artigue, L., Belt, S.T., 2017. Identification of di- and triterpenoid lipid tracers confirms the significant role of autoxidation in the degradation of terrestrial vascular plant material in the Canadian Arctic. Org. Geochem. 108, 43–50.
Ruescas, A., Hieronymi, M., Mateo-Garcia, G., Koponen, S., Camps-Valls, G., 2018. Machine learning regression approaches for colored dissolved organic matter (CDOM) retrieval with S2-MSI and S3-OLCI simulated data. Remote Sens. 10 (5), 786.
Ruhala, S.S., Zarnetske, J.P., 2016. Using in-situ optical sensors to study dissolved organic carbon dynamics of streams and watersheds: a review. Sci. Total Environ. 575, 713–723.
Sankar, M., Dash, P., Singh, S., Lu, Y., Mercer, A.E., Chen, S., 2019. Effect of photobiodegradation and biodegradation on the biogeochemical cycling of dissolved organic matter across diverse surface water bodies. J. Environ. Sci. 77, 130–147.
Scully, N.M., Cooper, W.J., Tranvik, L.J., 2003. Photochemical effects on microbial activity in natural waters: the interaction of reactive oxygen species and dissolved organic matter. FEMS Microbiol. Ecol. 46 (3), 353–357.
Shi, Y., Zhang, L., Li, Y., Zhou, L., Zhou, Y., Zhang, Y., Huang, C., Li, H., Zhu, G., 2020. Influence of land use and rainfall on the optical properties of dissolved organic matter in a key drinking water reservoir in China. Sci. Total Environ. 699, 134301.
Shiu, R.-F., Lee, C.-L., 2017. Role of microgel formation in scavenging of chromophoric dissolved organic matter and heavy metals in a river-sea system. J. Hazard. Mater. 328, 12–20.
Siegel, D., Maritorena, S., Nelson, N., Hansell, D.A., Lorenzi-Kayser, M., 2002. Global distribution and dynamics of colored dissolved and detrital organic materials. J. Geophys. Res. Oceans 107 (C12), 3228.
Singer, G.A., Fasching, C., Wilhelm, L., Niggemann, J., Steier, P., Dittmar, T., Battin, T.J., 2012. Biogeochemically diverse organic matter in Alpine glaciers and its downstream fate. Nat. Geosci. 5 (10), 710–714.
Sleighter, R.L., Hatcher, P.G., 2007. The application of electrospray ionization coupled to ultrahigh resolution mass spectrometry for the molecular characterization of natural organic matter. J. Mass Spectrom. 42 (5), 559–574.
Song, K., Zhao, Y., Wen, Z., Fang, C., Shang, Y., 2017. A systematic examination of the relationships between CDOM and DOC in inland waters in China. Hydrol. Earth Syst. Sci. 21 (10), 5127–5141.
Spencer, R.G.M., Aiken, G.R., Butler, K.D., Dornblaser, M.M., Striegl, R.G., Hernes, P.J., 2009. Utilizing chromophoric dissolved organic matter measurements to derive export and reactivity of dissolved organic carbon exported to the Arctic Ocean: a case study of the Yukon River, Alaska. Geophys. Res. Lett. 36 (6).
Spencer, R.G., Butler, K.D., Aiken, G.R., 2012. Dissolved organic carbon and chromophoric dissolved organic matter properties of rivers in the USA. Journal of Geophysical Research: Biogeosciences (2005–2012) 117 (G3). https://doi.org/10.1029/2011JG001928.
Spencer, R.G., Guo, W., Raymond, P.A., Dittmar, T., Hood, E., Fellman, J., Stubbins, A., 2014. Source and biolability of ancient dissolved organic matter in glacier and lake ecosystems on the Tibetan plateau. Geochim. Cosmochim. Acta 142, 64–74.
Stedmon, C.A., Bro, R., 2008. Characterizing dissolved organic matter fluorescence with parallel factor analysis: a tutorial. Limnology and Oceanography-Methods 6, 572–579.
Stedmon, C.A., Markager, S., 2005. Resolving the variability in dissolved organic matter fluorescence in a temperate estuary and its catchment using PARAFAC analysis. Limnol. Oceanogr. 50 (2), 686–697.
Stedmon, C.A., Markager, S., Kaas, H., 2000. Optical properties and signatures of chromophoric dissolved organic matter (CDOM) in Danish coastal waters. Estuar. Coast. Shelf Sci. 51 (2), 267–278.
Stedmon, C.A., Markager, S., Bro, R., 2003. Tracing dissolved organic matter in aquatic environments using a new approach to fluorescence spectroscopy. Mar. Chem. 82 (3–4), 239–254.

Stedmon, C.A., Markager, S., Tranvik, L., Kronberg, L., Slätis, T., Martinsen, W., 2007. Photochemical production of ammonium and transformation of dissolved organic matter in the Baltic Sea. Mar. Chem. 104 (3–4), 227–240.
Stedmon, C.A., Granskog, M.A., Dodd, P.A., 2015. An approach to estimate the freshwater contribution from glacial melt and precipitation in East Greenland shelf waters using colored dissolved organic matter (CDOM). J. Geophys. Res. Oceans 120 (2), 1107–1117.
Stubbins, A., Spencer, R.G., Chen, H., Hatcher, P.G., Mopper, K., Hernes, P.J., Mwamba, V.L., Mangangu, A.M., Wabakanghanzi, J.N., Six, J., 2010. Illuminated darkness: molecular signatures of Congo River dissolved organic matter and its photochemical alteration as revealed by ultrahigh precision mass spectrometry. Limnol. Oceanogr. 55 (4), 1467–1477.
Su, Y., Hu, E., Feng, M., Zhang, Y., Chen, F., Liu, Z., 2017. Comparison of bacterial growth in response to photodegraded terrestrial chromophoric dissolved organic matter in two lakes. Sci. Total Environ. 579, 1203–1214.
Sulzberger, B., Durisch-Kaiser, E., 2009. Chemical characterization of dissolved organic matter (DOM): a prerequisite for understanding UV-induced changes of DOM absorption properties and bioavailability. Aquat. Sci. 71 (2), 104–126.
Swan, C.M., Nelson, N.B., Siegel, D.A., Fields, E.A., 2013. A model for remote estimation of ultraviolet absorption by chromophoric dissolved organic matter based on the global distribution of spectral slope. Remote Sens. Environ. 136, 277–285.
Tranvik, L.J., Downing, J.A., Cotner, J.B., Loiselle, S.A., Striegl, R.G., Ballatore, T.J., Dillon, P., Finlay, K., Fortino, K., Knoll, L.B., 2009. Lakes and reservoirs as regulators of carbon cycling and climate. Limnol. Oceanogr. 54 (6), 2298–2314.
Tranvik, L.J., Cole, J.J., Prairie, Y.T., 2018. The study of carbon in inland waters—from isolated ecosystems to players in the global carbon cycle. Limnology and Oceanography letters 3 (3), 41–48.
Vähätalo, A.V., Wetzel, R.G., 2004. Photochemical and microbial decomposition of chromophoric dissolved organic matter during long (months–years) exposures. Mar. Chem. 89 (1–4), 313–326.
Vähätalo, A.V., Wetzel, R.G., 2008. Long-term photochemical and microbial decomposition of wetland-derived dissolved organic matter with alteration of ^{13}C: ^{12}C mass ratio. Limnol. Oceanogr. 53 (4), 1387–1392.
Wachenfeldt, E.v., Bastviken, D., Tranvika, L.J., 2009. Microbially induced flocculation of allochthonous dissolved organic carbon in lakes. Limnol. Oceanogr. 54 (5), 1811–1818.
Waggoner, D.C., Wozniak, A.S., Cory, R.M., Hatcher, P.G., 2017. The role of reactive oxygen species in the degradation of lignin derived dissolved organic matter. Geochim. Cosmochim. Acta 208, 171–184.
Ward, C.P., Nalven, S.G., Crump, B.C., Kling, G.W., Cory, R.M., 2017. Photochemical alteration of organic carbon draining permafrost soils shifts microbial metabolic pathways and stimulates respiration. Nat. Commun. 8 (1), 772.
Wear, E.K., Carlson, C.A., James, A.K., Brzezinski, M.A., Windecker, L.A., Nelson, C.E., 2015. Synchronous shifts in dissolved organic carbon bioavailability and bacterial community responses over the course of an upwelling-driven phytoplankton bloom. Limnol. Oceanogr. 60 (2), 657–677.
Weishaar, J.L., Aiken, G.R., Bergamaschi, B.A., Fram, M.S., Fujii, R., Mopper, K., 2003. Evaluation of specific ultraviolet absorbance as an indicator of the chemical composition and reactivity of dissolved organic carbon. Environ. Sci. Technol. 37 (20), 4702–4708.
Wen, Z., Song, K., Liu, G., Shang, Y., Fang, C., Du, J., Lyu, L., 2019. Quantifying the trophic status of lakes using total light absorption of optically active components. Environ. Pollut. 245, 684–693.
Williams, C.J., Yamashita, Y., Wilson, H.F., Jaffé, R., Xenopoulos, M.A., 2010. Unraveling the role of land use and microbial activity in shaping dissolved organic matter characteristics in stream ecosystems. Limnol. Oceanogr. 55 (3), 1159–1171.
Williams, C.J., Frost, P.C., Morales-Williams, A.M., Larson, J.H., Richardson, W.B., Chiandet, A.S., Xenopoulos, M.A., 2016. Human activities cause distinct dissolved organic matter composition across freshwater ecosystems. Glob. Chang. Biol. 22 (2), 613–626.
Williamson, C.E., Zepp, R.G., Lucas, R.M., Madronich, S., Austin, A.T., Ballaré, C.L., Norval, M., Sulzberger, B., Bais, A.F., Mckenzie, R.L., 2014. Solar ultraviolet radiation in a changing climate. Nat. Clim. Chang. 4 (6), 434–441.
Williamson, C.E., Overholt, E.P., Pilla, R.M., Leach, T.H., Brentrup, J.A., Knoll, L.B., Mette, E.M., Moeller, R.E., 2015. Ecological consequences of long-term browning in lakes. Sci. Rep. 5. https://doi.org/10.1038/srep18666.
Wilson, H.F., Xenopoulos, M.A., 2009. Effects of agricultural land use on the composition of fluvial dissolved organic matter. Nat. Geosci. 2 (1), 37–41.
Wolf, R., Heuschele, J., 2018. Water browning influences the behavioral effects of ultraviolet radiation on zooplankton. Front. Ecol. Evol. 6, 26.
Wu, F., Evans, R., Dillon, P., 2003. Separation and characterization of NOM by high-performance liquid chromatography and on-line three-dimensional excitation emission matrix fluorescence detection. Environ. Sci. Technol. 37 (16), 3687–3693.
Wünsch, U.J., Stedmon, C.A., Tranvik, L.J., Guillemette, F., 2018. Unraveling the size-dependent optical properties of dissolved organic matter. Limnol. Oceanogr. 63 (2), 588–601.
Wünsch, U.J., Bro, R., Stedmon, C.A., Wenig, P., Murphy, K.R., 2019. Emerging patterns in the global distribution of dissolved organic matter fluorescence. Anal. Methods 11 (7), 888–893.
Wymore, A.S., Potter, J., Rodriguez-Cardona, B., McDowell, W.H., 2018. Using in-situ optical sensors to understand the biogeochemistry of dissolved organic matter across a stream network. Water Resour. Res. 54 (4), 2949–2958.
Xiao, Y.H., Raike, A., Hartikainen, H., Vahatalo, A.V., 2015. Iron as a source of color in river waters. Sci. Total Environ. 536, 914–923.
Xu, H.C., Guo, L.D., 2018. Intriguing changes in molecular size and composition of dissolved organic matter induced by microbial degradation and self-assembly. Water Res. 135, 187–194.
Xu, J., Fang, C.Y., Gao, D., Zhang, H.S., Gao, C., Xu, Z.C., Wang, Y.Q., 2018. Optical models for remote sensing of chromophoric dissolved organic matter (CDOM) absorption in Poyang Lake. ISPRS J. Photogramm. Remote Sens. 142, 124–136.
Yan, M., Wang, D., Korshin, G.V., Benedetti, M.F., 2013. Quantifying metal ions binding onto dissolved organic matter using log-transformed absorbance spectra. Water Res. 47 (7), 2603–2611.
Zark, M., Dittmar, T., 2018. Universal molecular structures in natural dissolved organic matter. Nat. Commun. 9, 3178.
Zhang, Y., Xie, H., 2015. Photomineralization and photomethanification of dissolved organic matter in Saguenay River surface water. Biogeosciences 12, 6823–6836.
Zhang, Y., Liu, M., Qin, B., Feng, S., 2009a. Photochemical degradation of chromophoric-dissolved organic matter exposed to simulated UV-B and natural solar radiation. Hydrobiologia 627 (1), 159–168.
Zhang, Y., van Dijk, M.A., Liu, M., Zhu, G., Qin, B., 2009b. The contribution of phytoplankton degradation to chromophoric dissolved organic matter (CDOM) in eutrophic shallow lakes: field and experimental evidence. Water Res. 43 (18), 4685–4697.
Zhang, Y., Yin, Y., Feng, L., Zhu, G., Shi, Z., Liu, X., Zhang, Y., 2011a. Characterizing chromophoric dissolved organic matter in Lake Tianmuhu and its catchment basin using excitation-emission matrix fluorescence and parallel factor analysis. Water Res. 45 (16), 5110–5122.
Zhang, Y., Yin, Y., Liu, X., Shi, Z., Feng, L., Liu, M., Zhu, G., Gong, Z., Qin, B., 2011b. Spatial-seasonal dynamics of chromophoric dissolved organic matter in Lake Taihu, a large eutrophic, shallow lake in China. Org. Geochem. 42 (5), 510–519.
Zhang, Y., Yin, Y., Zhang, E., Zhu, G., Liu, M., Feng, L., Qin, B., Liu, X., 2011c. Spectral attenuation of ultraviolet and visible radiation in lakes in the Yunnan plateau, and the middle and lower reaches of the Yangtze River, China. Photochem. Photobiol. Sci. 10 (4), 469–482.
Zhang, Y., Liu, X., Osburn, C.L., Wang, M., Qin, B., Zhou, Y., 2013a. Photobleaching response of different sources of chromophoric dissolved organic matter exposed to natural solar radiation using absorption and excitation–emission matrix spectra. PLoS One 8 (10), e77515.
Zhang, Y., Liu, X., Wang, M., Qin, B., 2013b. Compositional differences of chromophoric dissolved organic matter derived from phytoplankton and macrophytes. Org. Geochem. 55, 26–37.
Zhang, Y., Gao, G., Shi, K., Niu, C., Zhou, Y., Qin, B., Liu, X., 2014. Absorption and fluorescence characteristics of rainwater CDOM and contribution to Lake Taihu, China. Atmos. Environ. 98 (32), 483–491.
Zhang, Y., Zhou, Y., Shi, K., Qin, B., Yao, X., Zhang, Y., 2018. Optical properties and composition changes in chromophoric dissolved organic matter along trophic gradients: implications for monitoring and assessing lake eutrophication. Water Res. 131, 255–263.
Zhao, J., Cao, W., Xu, Z., Ai, B., Yang, Y., Jin, G., Wang, G., Zhou, W., Chen, Y., Chen, H., 2018. Estimating CDOM concentration in highly turbid estuarine coastal waters. J. Geophys. Res. Oceans 123 (8), 5856–5873.
Zhou, Y., Zhang, Y., Jeppesen, E., Murphy, K.R., Shi, K., Liu, M., Liu, X., Zhu, G., 2016. Inflow rate-driven changes in the composition and dynamics of chromophoric dissolved organic matter in a large drinking water lake. Water Res. 100, 211–221.
Zhou, Y., Shi, K., Zhang, Y., Jeppesen, E., Liu, X., Zhou, Q., Wu, H., Tang, X., Zhu, G., 2017. Fluorescence peak integration ratio IC: IT as a new potential indicator tracing the compositional changes in chromophoric dissolved organic matter. Sci. Total Environ. 574, 1588–1598.
Zhou, Y., Davidson, T.A., Yao, X., Zhang, Y., Qin, B., 2018a. How autochthonous dissolved organic matter responds to eutrophication and climate warming: evidence from a cross-continental data analysis and experiments. Earth Sci. Rev. 185, 928–937.
Zhou, Y., Xiao, Q., Yao, X., Zhang, Y., Zhang, M., Shi, K., Lee, X., Podgorski, D.C., Qin, B., Spencer, R.G.M., Jeppesen, E., 2018b. Accumulation of terrestrial dissolved organic matter potentially enhances dissolved methane levels in eutrophic Lake Taihu, China. Environ. Sci. Technol. 52 (18), 10297–10306.
Zhou, L., Zhou, Y., Hu, Y., Cai, J., Liu, X., Bai, C., Tang, X., Zhang, Y., Jang, K.-S., Spencer, R.G., 2019. Microbial production and consumption of dissolved organic matter in glacial ecosystems on the Tibetan plateau. Water Res. 160, 18–28.
Zhu, W., Yu, Q., Tian, Y.Q., Chen, R.F., Gardner, G.B., 2011. Estimation of chromophoric dissolved organic matter in the Mississippi and Atchafalaya river plume regions using above-surface hyperspectral remote sensing. Journal of Geophysical Research: Oceans (1978–2012) 116 (C2).
Zhu, W., Yu, Q., Tian, Y.Q., Becker, B.L., Zheng, T., Carrick, H.J., 2014. An assessment of remote sensing algorithms for colored dissolved organic matter in complex freshwater environments. Remote Sens. Environ. 140, 766–778.
Zsolnay, A., Baigar, E., Jimenez, M., Steinweg, B., Saccomandi, F., 1999. Differentiating with fluorescence spectroscopy the sources of dissolved organic matter in soils subjected to drying. Chemosphere 38 (1), 45–50.